THE ESSENTIAL ROLE OF THE DEUBIQUITINATING ENZYME UBPY IN T CELL DEVELOPMENT AND FUNCTION

Dissertation zur Erlangung des akademischen Grades
Doktor der Naturwissenschaften,
Doctor rerum naturalium

eingereicht im Fachbereich Biologie, Chemie, Pharmazie
der freien Universität Berlin

vorgelegt von

Agnes Kisser
aus Wien

Berlin April 29, 2008

This work was executed at the Leibniz Institute for Molecular Pharmacology, Berlin, in the Department of Molecular Genetics under the supervision of Dr. Klaus-Peter Knobeloch and Prof. Dr. Ivan Horak.

Referees:

Prof. Dr. I. Horak, Department of Molecular Genetics, Leibniz Institute for Molecular Pharmacology, Berlin

Prof. Dr. H. Oschkinat, Department of NMR-supported Structural Biology, Leibniz Institute for Molecular Pharmacology, Berlin

Disputation date: 08 December 2008

Statement

Herewith, I declare that I prepared the presented dissertation myself and without the use of illegitimate aids. I used no other but the indicated sources and accessories. Further, I insure that this dissertation has not before been submitted to any other faculty for examination.

Berlin, April 29, 2008

(Agnes Kisser)

TO CHARLOTTE

Contents

List of Figures

Abbreviations

AMP	Adenosine monophosphate
AMSH	Associated molecule with the SH3 domain of STAM
ATP	Adenosine triphosphate
B7-2	CD86 molecule
BFA	Brefeldin A
BrdU	Bromodeoxyuridine
cbl	Casitas B-lineage lymphoma
CD	Cluster of differentiation
CFTR	Cystic fibrosis transmembrane conductance regulator
CHMP	Charged MVB proteins
CLASP	Clathrin-coat-associated sorting protein
CP	Core particle (26S ribosome)
CX	Cycloheximide
CXCR4	Chemokine (C-X-C motif) receptor 4
CYLD	Cylindromatosis gene product
DN	Double negative, CD4-CD8-
DNA	Deoxyribonucleic acid
DP	Double positive, CD4+CD8+
DUB	Deubiquitinating enzyme
DUBA	Deubiquitinating Enzyme A
EGFR	Epidermal growth factor receptor
eIF3	Eukaryotic initiation factor 3
ELISA	Enzyme-linked immunosorbent assay
ER	Endoplasmatic reticulum
ErbB3, ErbB4	v-erb-b2 erythroblastic leukemia viral oncogene homolog 3, 4 (avian)

ERK	Extracellular signal regulated kinase
ESCRT	Endosomal sorting complex required for transport
FACS	Fluorescence activated cell sorting
FoxP3	Forkhead Box P3
GADS	Grb2-Related Adaptor Downstream of Shc
GRAIL	Gene related to anergy in lymphocytes
Grb2	Growth factor receptor-bound protein 2
HECT	Homologous to the E6-AP Carboxyl Terminus
HGFR	Hepatocyte growth factor receptor
Hrs	Hepatocyte growth factor regulated tyrosine kinase substrate
HSA	Heat shock antigen
IκB	Inhibitor of NFκB
IBD	Inflammatory bowel disease
IFN	Interferon
IgG	Immune globulin G
IL	Interleukin
IL1R	Interleukin-1 receptor
IL2R	Interleukin 2 receptor
JAMM motif	JAB1/MPN/Mov34 metalloenzyme motif
KO	Knockout
LAT	Linker for activation of T cells
Lck	Lymphocyte-specific protein tyrosine kinase
loxP	locus of crossing over
MFI	Median fluorescence intensity
MHC	Major histocompatibility complex
MIT	Microtubule interacting and transport
MJD	Machado-Joseph-disease protein domain proteases
MLN	Mesenterial lymph nodes
MVB	Multivesicular body
NFκB	Nuclear factor κB
Nrdp1	Neuregulin receptor degradation protein-1
OTU	ovarian tumor
PBS	Phosphate buffered saline

PDGF(R)	Platelet-derived growth factor (receptor)
PE	Phycoerythrin
PI	Propidium iodide
PKCθ	Protein kinase Cθ
PLCγ1	Phospholipase Cγ1
rasGRF1	Ras protein-specific guanine nucleotide-releasing factor 1
RING	Really interesting new gene
RNA	Ribonucleic acid
RP	Regulatory particle (26S ribosome)
Rpn10	Non-ATPase base subunit of the 19S regulatory particle (RP) of the 26S proteasome
Rpn11	Metalloprotease subunit of the 19S regulatory particle of the 26S proteasome lid
SH3	Src homology 3
SP	Single positive, CD4+CD8- or CD4-CD8+
STAM	Signal transducing adapter molecule
Stat	Signal transducer and activator of transcription
TCR	T cell receptor
TGN	Trans-Golgi network
TLR	Toll-like receptors
TNF	Tumor necrosis factor
UBPY	Ubiquitin binding protease Y
UCH	Ubiquitin carboxy-terminal hydrolases
UIM	Ubiquitin interacting motif
USP	Ubiquitin-specific processing proteases
WT	Wildtype
Zap70	Zeta-chain-associated protein kinase 70

Chapter 1

Introduction

Ubiquitination was discovered in the late 1970's as an energy-dependent mechanism for intracellular protein breakdown [1, 2]. Soon it became clear that ubiquitin mediated degradation of proteins helps regulating such essential cellular mechanisms as cell cycle progression [3]. Today ubiquitination is known to be implicated in endocytosis and intracellular trafficking of proteins, in multiple signal transduction cascades and in the modulation of gene expression. This multifariousness of ubiquitin's functions places the molecule on a level with the well known regulator phosphate, which controls the activity of thousands of proteins.

While the enzymes responsible for the conjugation of ubiquitin to substrates have already extensively been studied, the role of the deubiquitinating enzymes (DUB) is only beginning to emerge. DUB are implicated in substrate unspecific processes such as recycling of ubiquitin from proteasome-targeted proteins and processing of ubiquitin precursors. In yeast, the only ubiquitin deconjugating enzyme necessary for viability is the metalloprotease Rpn11, responsible for ubiquitin recycling at the proteasome[4, 5]. In eukaryotes, however, substrate specific deubiquitination has a more essential role. The deubiquitinating enzyme A20 for example negatively regulates NFκB signaling and mice deficient for this enzyme die prematurely due to an

excessive inflammatory response [6]. In humans, a rare tumor of the skin appendages named cylindromatosis is caused by mutation of the ubiquitin peptidase CYLD [7].

The ubiquitin specific peptidase UBPY has first been described in 1998 as a growth-regulated isopeptidase [8]. The vital and non-redundant role of UBPY is demonstrated by the fact that the conventional knockout of UBPY is embryonically lethal [9]. Further studies with UBPY deficient cells revealed a function of UBPY in endocytic trafficking and stability of receptor tyrosine kinases [10, 11, 9]. Both mechanisms play a central role in T cell development and function. Since UBPY was also reported to interact with a major player in TCR signaling, the adaptor molecule GADS [12], and with a central regulator of T cell anergy, the E3 ligase GRAIL [13], this lead us to investigate the role of UBPY in T cells using a T cell specific knockout mouse model.

This introduction gives a general overview of the ubiquitin system in general and the deubiquitinating enzymes in detail. The present knowledge about UBPY is summarized. Finally, special emphasis is placed on the known functions of ubiquitination and deubiquitination in T cells.

1.1 Ubiquitination and deubiquitination

1.1.1 The ubiquitin molecule and the ubiquitination process

Ubiquitin is a small, heat-stable polypeptide of 76 amino acids that folds into a compact globular structure (Fig. 1.1). It can either be found in free form or covalently attached to target proteins via an isopeptide bond between the C-terminal glycine of ubiquitin and the ϵ-amino group of a lysine residue in substrate proteins. The ubiquitin molecule itself contains seven lysine residues at positions 6, 11, 27, 29, 33, 48 and 63,(referred to as K6, K11, K27...) through which

ubiquitin molecules can be linked to each other, leading to the formation of ubiquitin chains. The attachment of a single ubiquitin to a lysine residue of a substrate is defined as monoubiquitination, while polyubiquitinated substrates are modified by ubiquitin chains of four or more residues. Polyubiquitination can be further categorized according to the lysine residue used for chain formation. This variability of possible ubiquitin modifications explains how ubiquitination can regulate such a great diversity of processes in the cell.

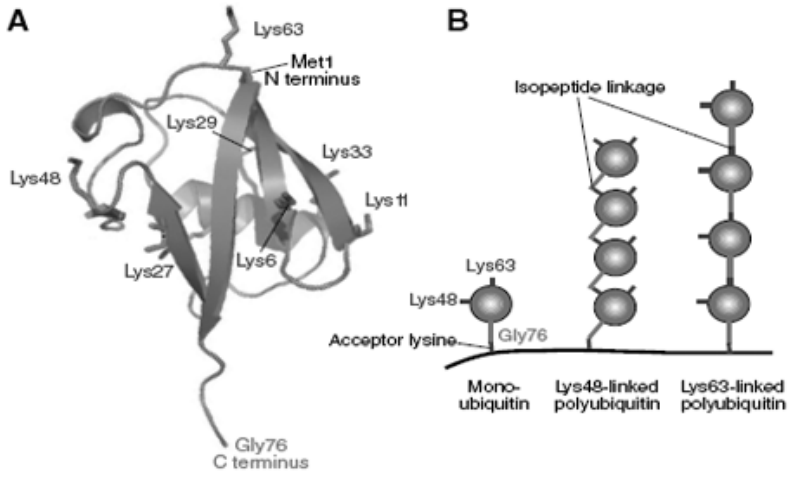

Figure 1.1: Ubiquitin, isopeptide linkage and chain conformation variations. (A) Ribbon diagram of the main chain of the ubiquitin molecule with the seven lysine residues in stick representation. Ubiquitin is a small, single domain protein of 76 residues consisting of a single anti-parallel β-sheet curved over an adjacent α-helix forming a highly stable, compact structure. The protruding C-terminus with the glycine 76 residue is used for isopeptide linkage of ubiquitin to a target lysine side chain. (B) Schematic representation of monoubiquitination, K48-linked and K63 linked polyubiquitination of target lysine residues. (Adapted from [14])

The attachment of ubiquitin to protein substrates occurs in a three-step process [2] depicted in Fig. 1.2. The first step consists in the energy-dependent activation of ubiquitin by an ubiquitin activating enzyme (E1). The E1 first uses ATP to produce an ubiquitin-adenylate intermediate. This intermediate is then transferred to the E1 active site cysteine residue with release of AMP, resulting in a thioester linkage between the C-terminal carboxyl group of ubiquitin and the E1

cysteine sulfhydryl group. In the second step, the ubiquitin is transferred from E1 to the active site cysteine of a ubiquitin-conjugating enzyme (E2) via a trans(thio)esterification reaction. The final step of the ubiquitination cascade is carried out by one of the hundreds of ubiquitin-protein ligases (E3). E3 enzymes usually contain one of two domains: a RING (Really interesting new gene) domain or a HECT (Homologous to the E6-AP Carboxyl Terminus) domain. RING E3 ligases mediate the transfer from E2 to substrate directly. In the case of HECT E3 ligases, a covalent E3-ubiquitin intermediate is formed before transfer of ubiquitin to the substrate protein [15].

While only two E1 enzymes were discovered so far in eukaryotes [16], the multiplicity of E2 and E3 enzymes enables target-specific ubiquitination. However some E3 ligases can modify more than one substrate and even perform different types of ubiquitination: the cbl E3 ligase for example is known to polyubiquitinate the Abl tyrosine kinase and monoubiquitinate EGFR. Thus, still other molecular factors are obviously needed to explain the correct timing, localization, type and specificity of ubiquitination.

1.1.2 Functions of ubiquitination

Tag for degradation through the proteasome

The ubiquitin-proteasome proteolytic pathway was the first function attributed to ubiquitination (reviewed in [15]). The presence of K48-linked ubiquitin chains of at least four residues on a protein targets this substrate for degradation in the 26S proteasome. The 26S proteasome is a 2,5MDa complex composed of the barrel-shaped 20S catalytic core particle (CP) and one or two 19S regulatory particles (RP). The RP is made up of two parts: the lid and the base. The polyubiquitin chains are recognized by the Rpn10, a subunit of the RP base. The proteasome

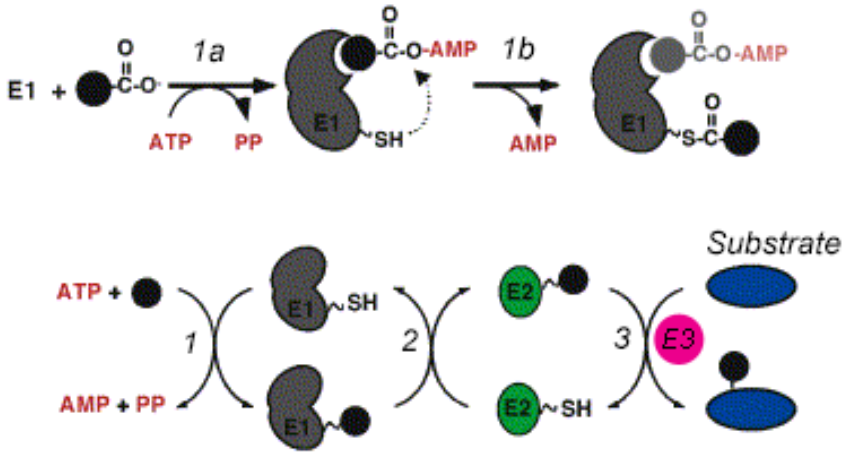

Figure 1.2: Ubiquitin is attached to a substrate by a three-step process. (1) Ubiquitin activation (1a) Formation of a ubiquitin-adenylate. (1b) Transfer of the ubiquitin-adenylate to the active site cysteine of the E1. (2) Transfer of the activated ubiquitin to the E2 enzyme. (3) E3-mediated transfer of ubiquitin to the substrate (adapted from [17]).

lid is a highly conserved complex related to the COP9 signalosome and the eukaryotic initiation factor 3 (eIF3)[18]. The most conserved lid component is the metalloprotease Rpn11, which removes the polyubiquitin chains from the substrates, enabling their further processing. The base contains the six proteasomic ATPases and attaches to the α-ring of the CP. These ATPases yield the energy necessary for unfolding of the substrate and opening of the proteasome channel, prerequisites for translocation of the substrate in the inner chamber of the CP. The CP is made of four heptameric rings: two outer identical α-rings and two inner identical β-rings. The β-particles harbor the protease active sites. At the inner site of the proteasome, the polypeptide is hydrolyzed by a nucleophilic mechanism, producing small peptide fragments. They are short-lived and do not accumulate in the cell, most likely due to rapid hydrolization by downstream proteases and aminopeptidases. Some of the peptides generated are transported through the endoplasmatic reticulum (ER) and are presented to the immune system by MHC (Major histocompatibility complex) class I molecules, making the proteasome a central component of the antigen presentation machinery.

Sorting signal in the biosynthetic and endocytotic pathways

Rather than in the 26S proteasome, membrane-bound proteins are disposed through the endosomal/ lysosomal pathway. This involves several ubiquitin-mediated trafficking steps that ultimately result in delivery of the proteins to the lysosome for degradation (Reviewed in [19], Fig. 1.3). First, ubiquitination mediates the internalization or endocytosis of proteins located in the plasma membrane and their targeting to early endosomes. At present it is thought, that the ubiquitin binding CLASPs (clathrin-coat-associated sorting proteins) epsin/eps15/eps15R recognize the ubiquitin endocytic sorting signal via their ubiquitin interacting motifs (UIM). Assembly of these CLASPs with phospholipids, AP-2, clathrin and each other then links the ubiquitinated cargo to the clathrin-dependent endocytic pathway [14]. Second, probably as a quality control mechanism, ubiquitination may also direct newly synthesized proteins from the trans-Golgi network to the early endosome.

At the endosome, ubiquitin mediated sorting into the lysosome is mediated by a vast network of protein-protein and protein-lipid interactions, whose central players are four highly conserved protein complexes, ESCRT-0, -I, -II and -III (Endosomal sorting complex required for transport) . The ESCRT complexes are responsible for cargo selection and the production of lumenal vesicles, resulting from inward budding of the endosomal membrane. This leads to the formation of the multi-vesicular body (MVB) or late endosome. Fusion of the MVB with the lysosome finally leads to proteolysis of vesicle lipids and proteins [19].

All of the ESCRTs except ESCRT-III recognize and bind the ubiquitinated cargo through diverse ubiquitin-interacting motifs. ESCRT-III lacks such modules, instead it recruits deubiquitinating enzymes and the ESCRT disassembly machinery. ESCRT-0 is composed of Hrs (Hepatocyte growth factor -regulated tyrosine kinase substrate) and STAM (signal transducing adaptor molecule). The two molecules interact constitutively with each other through coiled-coil domains

and expression of STAM is contingent to the presence of Hrs. Both ESCRT-0 components bind to clathrin leading to formation of Hrs-clathrin coats on endosomes, probably enabling thereby the encounter of ubiquitinated cargo with ESCRT-I [20]. Whereas depletion of Hrs leads to enlarged vacuolar structures with EGFR trapped at the membrane, depletion of the ESCRT-1 component TSG101 promotes the accumulation of EGFR and EGF on tubular clusters and induces the formation of multicisternal structures with an internal matrix (Review of the ESCRT machinery in [21]).

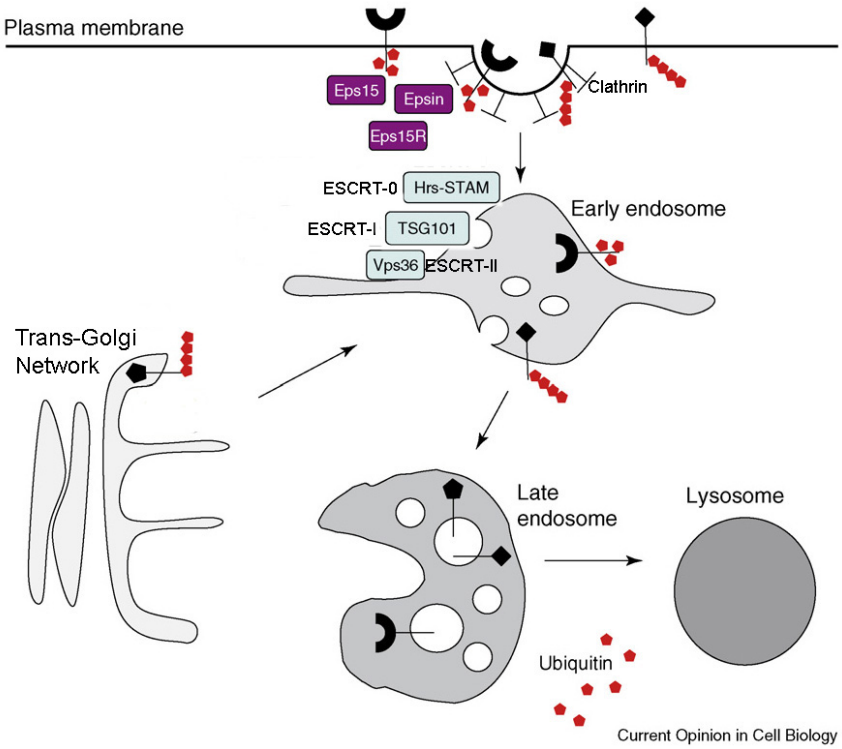

Figure 1.3: Proteins derived from the cell membrane or newly synthesized from the Golgi apparatus are tagged by ubiquitin (red) to direct them to early endosomes. During maturation towards late endosome, tagged membrane proteins destinated for degradation are sorted to lumenal vesicles, forming the so-called multivesicular body (MVB). The MVB/late endosome finally fuses with the lysosome, where the vesicles are degraded (Adapted from [19]).

The ubiquitin modifications involved in the lysosomal pathway are different to the K48 polyu-

biquitin chains targeting proteins to proteasomal degradation and exhibit great diversity ranging from single and multiple monoubiquitination to K63-linked diubiquitin or polyubiquitin chains. The current consensus view is that multiple ubiquitin residues increase the efficiency of sorting to the lysosomes, relatively independent of a particular conformation [19].

A major group of proteins regulated via the endosomal/ lysosomal pathway are signal- transducing receptors, including G protein coupled receptors (i.e. CXCR4), receptor tyrosine kinases (i.e. EGFR, PDGFR, HGFR/c-met), immune receptors (i.e. IL2R, T cell receptor, IgG receptor) and costimulatory molecules (i.e. B7-2). They are usually constantly internalized and recycled back to the cell membrane at a low rate. Upon stimulation receptor internalization and/or lysosomal degradation are accelerated leading to a downregulation of the plasma membrane signaling molecules. This mechanism regulates the signal length, receptor activity and mediates the termination of ligand-induced signaling.
Another group of proteins that undergo ubiquitin-mediated endocytosis are ion channels (i.e. CFTR) [20].

1.1.3 The deubiquitinating enzymes

Classes of deubiquitinating enzymes

The deubiquitinating enzymes (DUB) belong to the superfamily of proteases, which is classified according to the catalytic mechanism in aspartic, serine, threonine, metallo and cysteine proteases (reviewed in [5, 22]). DUB are found in the groups of metallo and cysteine proteases, with the majority of the DUB being cysteine proteases, whose enzymatic activity, by definition, relies on the thiol group of a cysteine residue in their active site.

This cysteine gets activated by deprotonation through an adjacent histidine residue. The now positively charged histidine is stabilized by a negatively charged residue, aspartate. These three amino acids constitute the catalytic triad of the cysteine proteases. During deubiquitination, the activated cysteine performs a nucleophilic attack on the carbonyl of the peptide bond between ubiquitin and its substrate. This generates an intermediate thiolester between the cysteine and the C-terminus of ubiquitin. Subsequently the histidine is deprotonated and the substrate released. The intermediate contains an oxyanion, that is stabilized by the so-called oxyanion hole, usually constituted by a aspartate, asparagine or glutamate residue together with the main chain of the catalytic cysteine. Finally, hydrolization of the thiolester intermediate regenerates free enzyme and ubiquitin.
In metalloproteases, in contrast, the active site residue is a zinc ion, that is stabilized by an aspartate and two histidines and binds and polarizes a water molecule for the nucleophilic attack.

According to sequence homologies and the structure of the catalytic domain, the DUB are divided in five subclasses.

1. USP (Ubiquitin-specific processing proteases)

   This is the largest subfamily of DUB with more than 50 members. The catalytic domain of the USP contains two short and conserved motifs called histidine and cysteine box with all the residues necessary for proteolysis. Beside the conserved motifs the catalytic domain may also contain large unrelated sequences probably with regulatory function. There is a great variability in length of the catalytic domain, from 300 to 800 amino acids.

   The USP evolutionary co-evolved with the E3 ligases, the enzymes responsible for target specificity of the ubiquitin conjugation, suggesting a close relationship between the two groups of enzymes [23].

2. The UCH (Ubiquitin carboxy-terminal hydrolases)

   This subclass has only four members identified so far. Structural and biochemical studies indicated that the active site of the UCH is partially covered by a loop, making it therefore difficult to access for substrates of more than 30 amino acids . Accordingly, UCH are thought to mainly play a role in ubiquitin salvage (the removal of small cellular nucleophiles) and in processing of newly synthesized ubiquitin [5].

3. The OTU(ovarian tumor)-related proteases

   This family of cysteine proteases has been predicted based on bioinformatical analyses [24]. Today 14 members of this subfamily are known. Their common feature is the ovarian tumor (OTU) domain. Structural analysis revealed that the OTU proteases do not have the complete catalytic triad of other cysteine proteases and instead use another mechanism, involving a hydrogen bonding network [25].

   The physiological function of only a few members is known. A20 is a specific feedback inhibitor of NFκB activation in the tumor necrosis factor (TNF), interleukin-1, and Toll-like receptor (TLR) pathways. The enzyme is exceptional in its dual enzymatic activity: while its N-terminal domain deubiquitinates K63-linked polyubiquitinated signaling mediators such as TRAF6 and RIP, its C-terminal domain acts as a ubiquitin ligase (E3) for K48-linked degradative polyubiquitination of the same substrates [26]. Also another member of the family, DUBA (Deubiquitinating enzyme A), is involved in innate immune responses. The enzyme negatively regulates the production of type I Interferon (IFN) by removing K63-linked polyubiquitin chains from the E3 ligase TRAF3 [27].

4. The Machado-Joseph disease protein domain proteases (MJD)

   This family was discovered by a bioinformatics search for other families of ubiquitin deconjugating enzymes[28]. So far the only known members are Ataxin-3 and some Ataxin-3

like proteins. The Machado-Joseph disease is a neurological disease, that is caused by a misfolded form of the Ataxin-3 protein. There are no homologues for MJD in yeast. Other biological functions of the MJD are not determined so far.

5. The JAMM/MPN+ proteases

   This family has been predicted on the basis of a shared JAB1/MPN/Mov34 metalloenzyme (JAMM) motif [29], with the consensus sequence Glu-X_nHis-X-His-X10-Asp. This motif contains two absolutely conserved histidine residues and one aspartic acid residue that coordinate together a zinc ion essential for the proteolytic activity [30]. The POH1 metalloprotease (Rpn11 in yeast) is part of the proteasome 19S regulatory subunit. Another member of this family is AMSH (Associated molecule with the SH3 domain of STAM). AMSH is found in a complex with STAM and Hrs at the endosomes. The enzyme has a strong specificity for K63-linked ubiquitin chains and is supposed to be involved in endosomal sorting [31].

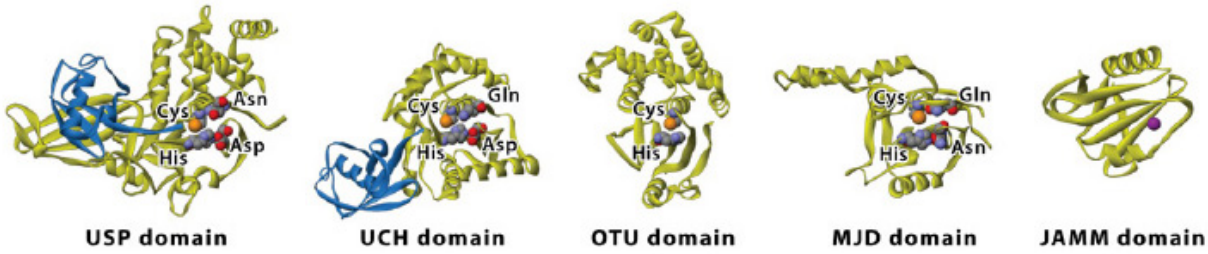

Figure 1.4: Structures of the catalytic domains of the five subclasses of deubiquitinating enzymes (Yellow) with ubiquitin (blue). Catalytic centers are shown as Van der Waals spheres: gray-carbon, blue-nitrogen, red-oxygen, orange-sulfur, purple-zinc (from [22].)

Despite the obvious sequence differences between the USP and UCH families of DUB, crystallographic analyses revealed that the three-dimensional structure of the catalytic core of both groups

of enzymes are nearly similar to each other and close to that of classical cysteine proteases. Interestingly, without ubiquitin-binding, the active sites of these enzymes are in catalytically inactive conformations. Ubiquitin-binding then induces a conformational change which either removes steric obstructions in the active site or brings the catalytic residues in the proper positions. This ubiquitin-dependent activation explains the specificity of the deubiquitinating enzymes for removal of ubiquitin and ubiquitin-like molecules from protein substrates [5].

Functions of deubiquitinating enzymes

The common feature of all deubiquitinating enzymes is their capacity to cleave ubiquitin-linked molecules after the C-terminal glycine residue of ubiquitin [32]. This property is necessary for a variety of cellular mechanisms, reviewed in [5].

1. Processing of ubiquitin precursors

   Ubiquitin is always synthesized in an inactive precursor form with a C-terminal extension beyond the terminal glycine [33]. This extension can result from coupling of the ubiquitin to ribosomal proteins or from the formation of ubiquitin multimers (in a head to tail manner, not to confuse with the ubiquitin chains that are linked through internal lysine residues). In either case the bond to be cleaved is a normal peptide bond. Activated ubiquitin is susceptible for nucleophilic attack by small molecules such as glutathione and polyamine. Because some of these components are present in quite high numbers in the cell, DUB are necessary to prevent ubiquitin to be titrated by these molecules. So far it is not yet exactly defined which DUB are responsible for cleavage of which kind of ubiquitin conjugates.

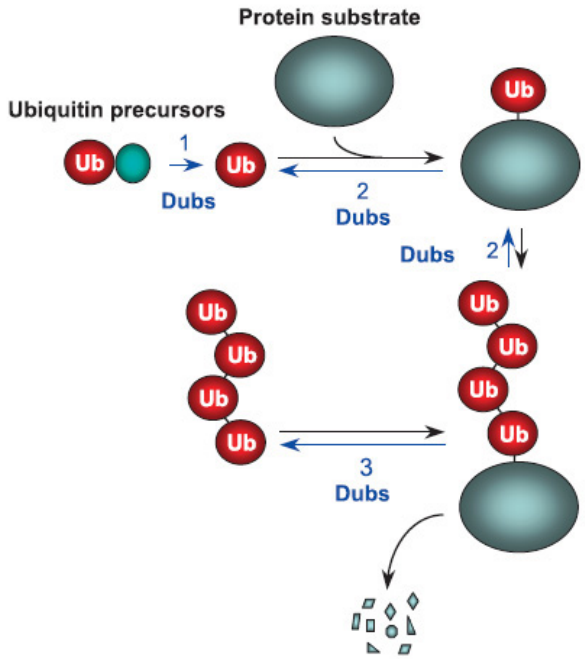

Figure 1.5: Functions of deubiquitinating enzymes. (1) Precursor processing. (2) Editing/ Rescue of ubiquitin substrates. (3) Ubiquitin recycling (adapted from [5]).

2. Rescue of ubiquitin substrates

   DUB can have a role in editing and rescue of ubiquitin conjugates, in order to ensure the specificity of ubiquitination. In that case, proteins have a general susceptibility for deubiquitination by the editing DUB and their level of ubiquitination can be enhanced by inhibiting the activity of DUB, allowing a second level of regulation. Plus, this creates a time window for ubiquitination to take its effect, before the protein returns to a deubiquitinated state. The degradation by the proteasome for example requires ubiquitin chains of at least four residues to be attached to the substrate [34]. A constant deubiquitination rate ensures that proteins with longer ubiquitin chains have a higher probability to be degraded than inappropriately tagged substrates with just little more than four ubiquitins. One ex-

ample of such an editing deubiquitinating enzyme is UCH37, a intrinsic subunit of the 19S proteasome subunit [35].

3. Ubiquitin recycling

   After targeting proteins to the proteasome the ubiquitin chains are cleaved off to prevent ubiquitin itself to be degraded and to recycle it in the cellular pool of free ubiquitin. Two DUB are supposed to be involved in this process. UBP6(USP14) is associated with the regulatory subunit of the 26S proteasome and its activity is strongly enhanced by proteasome binding. The metalloprotease Rpn11 (POH1 in mammalian cells) is the only DUB essential for viability in yeast [4]. Its activity in the context of the 26S proteasome is ATP dependent, probably it is coupled to the activity of ATPases that unfold and translocate protein substrates in the proteasome. Wilkinson *et al.* suggested that in mammalian cells, the enzyme responsible for ubiquitin chain disassembly is isopeptidase T[36].

   Naturally an ubiquitin recycling mechanism is also necessary for the second protein degradation machinery, the endosomal/lysosomal pathway. In yeast, the DUB involved in this process is supposed to be Doa4, which is localized to the endosomes and recycles ubiquitin from substrates already committed to inclusion to lumenal vesicles. Lack of Doa4 leads to exhaustion of the cellular pool of free ubiquitin and can be rescued by provision of additional ubiquitin [37].

1.2 UBPY

1.2.1 General facts

UBPY is a 1118 amino acids (human) or 1080 amino acids(mouse) protein. The first detailed description of the human UBPY was done by Naviglio et.al in 1998[8], three years later the mouse homologue was described by Gnesutta *et al.*[38]. The human UBPY is a 130kDa protein, while the mouse UBPY is of about 120kDa. The mouse and human sequences are highly homologous (Fig.1.6). Notably in the C-terminal region with the cysteine and histidine boxes characteristic for USP the homology is very high (97 %identity) . The genomic locus of the gene consists of at least 19 exons, with the second bearing the start codon and is located on chromosome 2 in mouse and chromosome 15 in humans. The mouse UBPY protein was found in a variety of tissues at low levels, with strongest expression in brain and testis [38]. The deubiquitinating activity of UBPY was tested in rabbit reticulocyte lysate [8] and mouse testis extracts pretreated with N-methylmaleimide to inhibit endogenous DUB activity [38], which confirmed that UBPY is able to deubiquitinate high molecular weight substrates. The enzyme has also been shown to cleave linear ubiquitin multimers [8]. UBPY is able to breakdown K48 and K63 linked ubiquitin chains [39, 40]. The mouse UBPY protein contains several functional regions depicted in Fig. 1.6:

- Two coiled-coil domains(93-142; 465-547).
- A rhodanese domain (185-310). Rhodanese domains are structural modules conserved from bacteria to human. Some may contain sulfurtransferase activity, but the UBPY rhodanese domain is catalytically inactive. The domain mediates interaction of UBPY with the E3 ligase Nrdp1 *(neuregulin receptor degradation protein 1)*[41].
- Two SH3 (Src homology 3) binding motifs with the consensus sequence *PX(V/I)(D/N)RXXKP*. These motif were identified by binding studies with the SH3 domain of STAM. It also binds

to the C-terminal SH3 domain of Grb2 (Growth factor receptor-bound protein 2), but, for example, not the N-terminal SH3 domain of Grb2 [42].

- The carboxy-terminal catalytic domain spanning amino acids 736-1068 with the cysteine box(740-758) and histidine box(1013-1032) characteristic for ubiquitin specific proteases.
- A 14-3-3 binding motif with consensus sequence RSYS^{680}SP at amino acid positions 677-682.
- A predicted MIT (microtubule interacting and transport) domain at amino acid positions 32-112.

1.2.2 Interaction partners of UBPY

Naviglio *et al.* showed that altering the amount of UBPY in U2OS cells led to dramatic changes in overall protein ubiquitination [8]. This implicates that UBPY is responsible for a key step in ubiquitin processing and/or deubiquitinates a broad spectrum of substrates.

A number of UBPY interaction partners has already been identified. The first reported binding partner of UBPY is the brain specific ras guanine exchange factor rasGRF-1(Ras protein-specific guanine nucleotide-releasing factor 1)[38]. Guanine exchange factors are responsible of the exchange of Guanine nucleotides (GDP/GTP) on Ras proteins and important factors in ras/raf signal transduction.

UBPY was further found in a trimolecular complex with GRAIL and otubain-1 [13]. GRAIL(gene related to anergy in lymphocytes) is an E3 ligase undergoing autoubiquitination. The interaction with UBPY stabilizes the protein.

UBPY also interacts with Nrdp1 *(neuregulin receptor degradation protein 1)* [41], an E3 ligase responsible for maintenance of steady state levels of the neuregulin receptor tyrosine kinases

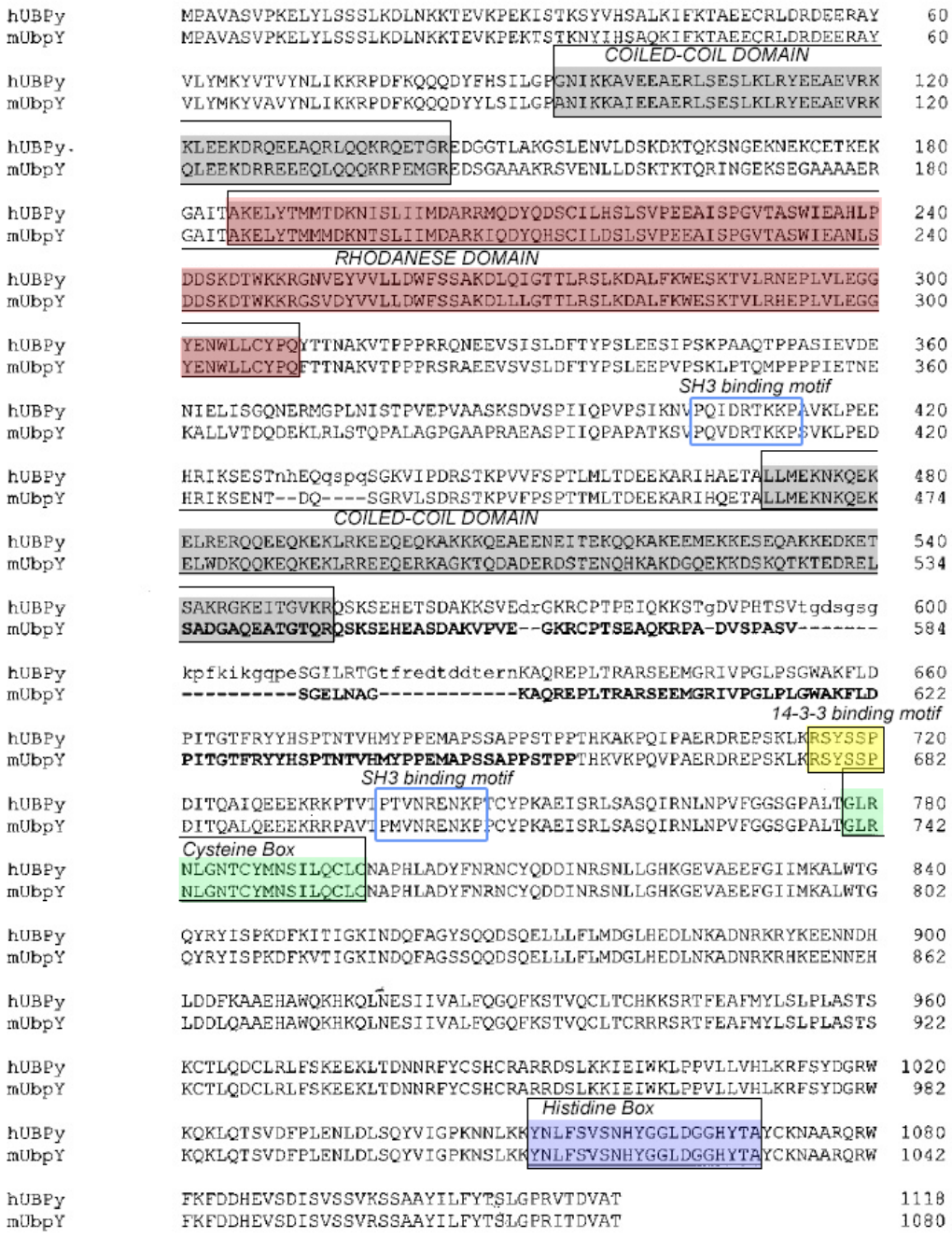

Figure 1.6: Alignment of the mouse and human UBPY amino acid sequence with the main functional domains(adapted from [38]).

ErbB3 and ErbB4. Mutational analysis revealed that the rhodanese and catalytic domain of UBPY are necessary for Nrdp1 binding. The protein undergoes autoubiquitination mediating its degradation unless stabilized by UBPY.

UBPY cDNA was also isolated in a screen for proteins binding to the SH3 domain of STAM [42]. STAM is tightly associated with Hrs through a coiled-coil motif. Deletion of either the coiled-coil motif or the SH3 domain of Hrs leads to defective degradation of PDGF and its receptor. Usually SH3 domains bind to proline-rich peptides containing the core sequence *PXXP*. Although UBPY contains six of such proline-rich sequences, the interaction with the STAM SH3 domain is mediated through two other, unusual SH3 binding domains.

In the same study *in vitro* binding assays showed that murine UBPY binds to the C-terminal SH3 domain of Grb2 (growth factor receptor bound protein 2). Grb2 is an adaptor protein that binds the epidermal growth factor receptor and contains one SH2 and two SH3 domains.

UBPY was also detected in a search for proteins binding to GADS [12]. Both GADS and Grb2 bind to phosphorylated LAT (Linker for activation of T cells) after TCR stimulation and are crucial elements in TCR signaling [43].

Three independent studies identified UBPY as an interaction partner with 14-3-3 proteins [44, 45, 46] through the 14-3-3 binding motif RSYS^{680}SP at amino acid positions 677-682. 14-3-3 proteins function at several key points in G(1)/S- and G(2)/M-transition by binding to regulatory proteins and modulating their function. The association with 14-3-3 proteins usually requires a specific phosphorylation of the protein ligand and mediates cell cycle arrest [47]. In the case of UBPY, binding is regulated by phosphorylation of the serine residue at position 680 [48]. Binding of 14-3-3 proteins to UBPY reduced its enzymatic activity. This could either be explained by a binding induced conformational change or, with the cysteine box only 60 amino acids downstream of the binding motif (Fig.1.6), a masking of the catalytic domain.

A recent study identified UBPY as an interaction partner with several CHMP (charged MVB

proteins) proteins, which are part of the endosomal ESCRT machinery [39]. Binding to these proteins is conferred by the MIT domain of UBPY.

1.2.3 The role of UBPY in cell proliferation

The first reported function of UBPY was described by Naviglio *et al.*. They observed that UBPY levels drop after growth inhibition through cell to cell contact or serum starvation and increase after restimulation, suggesting a role of UBPY in cell proliferation. This was further confirmed by knockout and knockdown models which consistently found that cells depleted of UBPY stop to proliferate and undergo growth arrest [8, 9]. More recent findings showed that UBPY is enzymatically inactivated through the binding of 14-3-3 proteins in a cell cycle dependent manner [48]. In a proteomic search, the binding of 14-3-3ζ to UBPY was detected only in interphasic, but not in mitotic cells [45]. Accordingly, Mizuno *et al.* showed that in cells treated with nocodazole, which arrests them in prometaphase, the 14-3-3 binding motif gets dephosphorylated, UBPY dissociates from 14-3-3 and is enzymatically activated [48]. For now it is not clear why UBPY gets specifically activated during early mitosis, especially in regard of its role in endosomal trafficking.

1.2.4 UBPY as a regulator of endosomal trafficking

A number of studies involving UBPY-depleted cells revealed an important role of UBPY in endosomal trafficking. All related work groups observed that UBPY knockdown or knockout leads to marked differences in endosomal morphology [49, 10, 11, 9]. Endosomes in all stages from early recycling endosome to lysosome are drastically enlarged and form unusual aggregates. Another clear effect of UBPY depletion is the accumulation of ubiquitinated substrates and more precisely of polyubiquitinated substrates. These ubiquitinated proteins colocalize with the en-

larged endosomes [10, 11, 9].

Two studies detected a (at least partial) loss of Hrs and complete loss of STAM [10, 9] in UBPY depleted cells. Hrs and STAM together form the ESCRT-0 complex located on early endosomes and responsible for endosomal trafficking. In cells depleted of Hrs or of both STAM isoforms ligand-induced EGFR degradation is impaired. According to that three studies also found impaired EGFR degradation in UBPY knockdown cells [10, 49, 50]. In these studies, EGFR accumulates in the cell and colocalizes with the enlarged early endosomes after EGF stimulation. In contrast, a previous study reported accelerated EGFR degradation in UBPY depleted cells [40] and immunohistochemical staining of EGFR in liver sections from UBPY knockout mice revealed that *in vivo* the EGFR is absent in most cells and displays intracellular localization in the few EGFR-positive cells. These apparently conflicting results led to two contradictory hypotheses concerning the role of UBPY in EGFR degradation. One attributes a stabilizing role to UBPY, where loss of UBPY leads to increased ubiquitination and thereby increased targeting of the receptor for lysosomal degradation. The other hypothesis establishes a functional homology of UBPY to the the yeast Doa4 deubiquitinating enzyme responsible for ubiquitin recycling at the vacuole. However, a defect in ubiquitin recycling would be accompanied by a depletion of the cellular pool of free ubiquitin, which is not the case in UBPY knockout cells [9].

1.3 Role of ubiquitination and deubiquitination in T cells

Covalent modification of proteins by Ubiquitin represents an essential regulatory mechanism that controls protein stability and a wide variety of molecular processes ranging from localization and transport of proteins to the modulation of signaling cascades and inter- and intramolecular protein interactions [51]. Thus it is not surprising that ubiquitination is of fundamental importance

in the regulation of the adaptive and innate immune system (for a recent review see [52]). In the last years, several components of the ubiquitin modification machinery have been shown to have substantial roles in the control of T cell development and differentiation, maintenance of immune tolerance and TCR signal transduction.

1.3.1 Thymocyte development and central tolerance

During thymocyte development, T cells are selected according to the interaction of their TCR with antigen/MHC molecules leading to activation of intracellular signal cascades. The strength and kinetics of these signaling responses determine whether T cells survive or are actively deleted, by positive and negative selection respectively. Thymocytes that are successfully selected pass beyond the double positive cd4+cd8 stage and mature into single positive cd4+ or cd8+ cells. Thymocytes from mice deficient for the E3 ligase c-cbl show enhanced and prolonged signaling through the TCR, leading to enhanced positive selection of CD4+thymocytes in MHC-classII restricted TCR transgenic mice [53, 54]. In contrast, thymocytes from mice deficient for the deubiquitinating enzyme CYLD show a reduced signaling through the TCR, leading to a developmental block at the double positive stage of thymocyte development. CYLD positively regulates a proximal step of TCR signaling, namely the recruitment of active Lck to its substrate, Zap70 [55]. CYLD deficient mice have hyperresponsive peripheral T cells mediating the spontaneous development of intestinal inflammation [56].

1.3.2 Peripheral tolerance

Thymocyte selection is one pathway through which the immune system establishes tolerance towards self-antigen. However, many self-antigens are first encountered by T cells only out-

side the thymus. In that case peripheral tolerance towards these self-antigens is established by several mechanisms including activation-induced cell death, suppression by regulatory T cells and anergy induction. T cells are rendered anergic by TCR stimulation without appropriate co-stimulation, leading to a sustained calcium signaling. Instead of being activated, the anergized T-cells fall into a state of unresponsiveness [57], characterized by the inability to produce IL-2 after restimulation with the antigen. The first E3 ligase that was linked to the induction of a clonal anergy state was c-CBL [58]. However c-cbl deficient mice fail to develop spontaneous autoimmune disease which is most likely explained by a compensatory function of the homologue CBL-B. CBL-B negatively regulates T-cell signaling by mediating the ubiquitination of the p85 subunit of Phosphoinositol-3-kinase (PI3K) which prevents its recruitment to the CD28 costimulatory molecule [59]. Consequently cells lacking CBL-B do not require costimulation by CD28 to mount a maximum IL-2 response and mice lacking CBL-B develop autoimmune disease [60, 61]. Several other E3 ligases are upregulated as a consequence of the sustained calcium signaling triggered by anergizing TCR signals, such as GRAIL, ITCH and Nedd4 [62]. These E3 ligases downmodulate the function of signaling molecules essential for T cell activation such as phospholipase Cγ1 (PLCγ1) and protein kinase Cθ (PKCθ). This leads to a block in downstream signaling pathways that are essential for IL-2 production and T-cell proliferation. Consistent with an essential role in anergy induction mice deficient for ITCH or CBL-b develop severe autoimmune disease [63, 61].

1.3.3 T cell receptor downmodulation

The TCR is a large multisubunit complex composed of at least eight subunits: TCR$\alpha\beta$, cd3$\epsilon\delta$, cd3$\epsilon\gamma$ and cd3$\zeta\zeta$. In resting T cells, the T cell receptor (TCR) is constitutively internalized through endocytosis. Constant surface levels of the receptor are maintained by its rapid recy-

cling back to the plasma membrane [64]. Following TCR-mediated stimulation, the entire TCR complex is internalized and all of its components are rapidly degraded in lysosomes[65] leading to a state of unresponsiveness for new antigenic stimuli of the T cell for 72hours or longer [66]. In case of the cd3-ζ chain, lysosomal degradation is mediated by ubiquitination through the E3 ligase cbl [67]. The interaction of c-cbl with the TCR is mediated by Zap-70 [67] and SLAP [68] The importance of this process was shown by a double knockout of c-cbl and cbl-b leading to development of hyperresponsive T cells, whose inability to downregulate TCR resulted in a lethal, probably autoimmune disease [69]. TCR levels are not only modulated in mature cells after antigenic stimulation, they are also developmentally regulated. At the CD4+CD8+ double-positive stage of development, thymocytes have a strict requirement for signals through the TCR for both positive and negative selection. The TCR expression at that stage is only 10% of the expression on single positive thymocytes and peripheral T cells [70]. The active maintenance of low surface TCR expression probably decreases their sensitivity for interactions with self peptide - MHC molecules so that quantitative differences in signaling can be distinguished more accurately. In immature thymocytes the rate of TCR assembly is kept low due to high degradation rates of newly synthesized TCR α chains. C-cbl deficient thymocytes exhibit higher levels of TCR, independently of TCR triggering [53]. It is conceivable that the developmental regulation of degradation rates might be mediated by regulation of the ubiquitination machinery.

1.3.4 NFκB signaling

One of the first immune responses that was shown to depend on ubiquitination is NFκB (Nuclear factor kappa B) activation(reviewed in [52]). Several immune receptors can trigger NFκB activation: TCR, TLR, TNFR, IL1R . Ligand binding causes phosphorylation of the inhibitory molecule IκB, complexed with the NFκB dimers. Phosphorylated IκB is recognized by a SCF

complex which mediates K48-polyubiquitination of IκB. Ubiquitinated IκB is degraded in the proteasome, the liberated NFκB dimer enters the nucleus where it initiates transcription of NFκB target genes. Phosphorylation of IκB is equally dependent of an ubiquitination process. Triggering of the receptors activates the E3 ligase TRAF6 which mediates K63 ubiquitination of NEMO, a subunit of the IκB kinase complex (IKK). This activates the IKK complex enabling it to phosphorylate IκB (Fig.1.7).

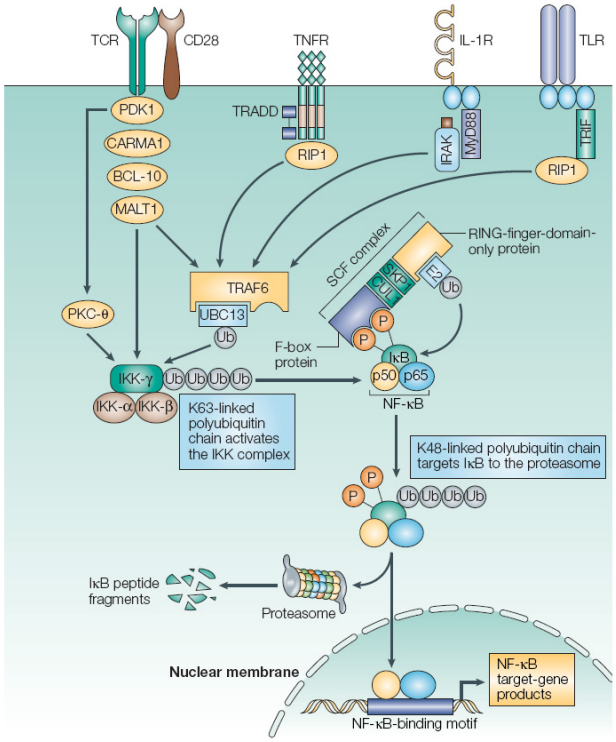

Figure 1.7: Ubiquitin mediated NFκB activation(from [52]).

Chapter 2

Aim of the project

The importance of ubiquitin deconjugation for T-cell function was demonstrated only recently by the analysis of mice deficient for the ubiquitin carboxy-terminal hydrolase CYLD. Two independent studies showed that T cells derived from CYLD knockout mice display a hyperresponsive phenotype and that CYLD deficient mice spontaneously developed intestinal inflammation [56] or were more susceptible to induced colonic inflammation [71]. The role of CYLD as negative regulator of NFκB activation was already well established *in vitro* [72, 73, 74], however only the study of the knockout mouse models allowed to discern cell-type specific targets of the enzyme within the NFκB pathway such as Lck in thymocytes [55] and Tak1 in mature T cells [56], emphasizing the importance of mouse models for the understanding of protein function especially in the context of the immune system.

The deubiquitinating enzyme UBPY has an essential role in endocytic trafficking and ligand-induced downmodulation of receptor tyrosine kinases [10, 11, 9]. The correct regulation of TCR downmodulation after ligand stimulation is essential for maintenance of immune homeostasis [69] and intracellular compartmentalization of TCR signaling components is proposed to determine selection outcome in thymocytes [75]. UBPY was also reported to interact with a major

player in TCR signaling, the adaptor molecule GADS [12], and with a central regulator of T cell anergy, the E3 ligase GRAIL [13]. These results suggested a potential role of UBPY in T cell function. As the conventional knockout of UBPY is embryonically lethal and induced deletion in mature animals causes rapid death of the animals [9], cre/LoxP mediated targeting was used to generate mice lacking UBPY specifically in T cells.

In these mice the UBPY gene is deleted during the CD4-CD8- double negative stage 3 of thymocyte development, yielding UBPY deleted T cells of all later stages, from CD4+CD8+ double positive thymocytes to mature CD4+ and CD8+ T lymphocytes. Using this mouse model, the present work aimed to clarify the following questions: What is the consequence of T-cell specific deletion of UBPY in the context of the hole organism? Is UBPY in T cells required for a functional immune system and do T cells normally develop in the absence of UBPY? Are UBPY-deficient T cells functional in response to antigen stimulation and anergy induction? Is UBPY involved in intracellular trafficking of the TCR or in the signal transduction events triggered by TCR stimulation?

Chapter 3

Materials

3.1 Reagents and chemicals

Acrylamide (30%) Bisacrylamide (0.8%)	Roth, Karlsruhe, Germany
Agarose NEEO	Roth, Karlsruhe, Germany
Ammonium persulfate (APS)	Sigma-Aldrich, Steinheim, Germany
Bromphenol Blue	Sigma-Aldrich, Steinheim, Germany
Bovine serum albumine (BSA)	AppliChem GmbH, Darmstadt, Germany
Brefeldin A	Sigma-Aldrich
Chlorophorm	Merck, Darmstadt, Germany
Complete protease inhibitor cocktail tablets (PIT)	Roche, Mannheim, Germany
Cycloheximide	Sigma-Aldrich, Steinheim, Germany
DNA from salmon sperm	Sigma-Aldrich, Steinheim, Germany
dNTPs (10mM)	MBI Fermentas, St.Leon Rot, Germany
α-^{32}P dCTP (3000 Ci/mmol)	Amersham Biosciences, Munich, Germany
Ethanol, 99%	Merck, Darmstadt, Germany
Ethidium bromide	Sigma-Aldrich, Steinheim, Germany
L-glutamine (200mM, sterile)	Gibco, Invitrogen, Karlsruhe,Germany

Immobilon^{TM}Western Chemilumineszenz HRP Substrat	Millipore
Isoamylalcohol, 98%	Roth, Karlsruhe, Germany
Isopropanol	Roth, Karlsruhe, Germany
2-mercaptoethanol (50mM, sterile)	Gibco, Invitrogen,Karlsruhe,Germany
Magnesium dichloride ($MgCl_2$)	MBI Fermentas, St.Leon Rot, Germany
Methanol, 99%	Roth, Karlsruhe, Germany
Phenol	Roth, Karlsruhe, Germany
Ponceau S	Sigma-Aldrich, Steinheim, Germany
Polyoxyethylensorbitanmonolaurat (Tween 20)	Sigma-Aldrich, Steinheim, Germany
Propidium iodide (PI)	Sigma-Aldrich, Steinheim, Germany
Roti®Nanoquant	Roth, Karlsruhe, Germany
Sodium azide (NaN_3)	Sigma-Aldrich, Steinheim, Germany
Sodium chloride (NaCl)	Roth, Karlsruhe, Germany
Sodium hydroxide (NaOH)	Roth, Karlsruhe, Germany
Sodium lauryl sulphate (SDS)	Sigma-Aldrich, Steinheim, Germany
Sodium hydrogenphosphate ($NaPO_2$)	Roth, Karlsruhe, Germany
methyl-^{3}H-thymidine	Amersham Biosciences, Munich, Germany
Tetra-methyl-ethylenediamine (TEMED)	Gibco, Invitrogen,Karlsruhe,Germany
Tris (hidroxymethyl) aminomethan (Tris)	Roth, Karlsruhe, Germany

3.2 Buffers and solutions

When not otherwise stated, deionised (Millipore) water was used as solvent.

Annexin V staining buffer (10x)	0.1M Hepes (pH 7.4), 1.4M NaCl, 25mM CaCl2
APS solution	10% APS in water, prepared fresh
BD PharmLyse^{TM} erythrocyte lysis buffer 10x	BD Biosciences, Pharmingen, Karlsruhe, Germany
Blocking solution (Western blotting)	5% low-fat milk in TBS, 0.1% Tween 20 or 3%BSA in TBS-T, 0.1%NaN_3

CasyTon® isotonic buffer	Scharfe System, Reutlingen, Germany
Denhardt's solution	2% (w/v) BSA; 2% Ficoll; 2% Polyvinylpyrrolidon
DNA loading buffer	10x 0.4% Bromphenol Blue; 0.4% xylencyanol; 50% glycerol; 0.1M EDTA
DNA lysis buffer	50mM Tris pH 8,0; 100mM EDTA; 100mM NaCl; 1% SDS; 400μg/ml Proteinase K;
Electrophoresis buffer	25mM Tris; 250mM glycine, pH 8.3; 0.1% SDS
FACS buffer	2% FCS, 2mM EDTA; 0.1% NaN3 in PBS
PBS	PAA Laboratories, Pasching, Germany
PCR buffer	Bioline, Luckenwalde, Germany
Ponceau S stain	0.1% Ponceau S in 5% acetic acid
Pre-hybridization solution (Southern)	5xSSC; 0.5% SDS; 100μg salmon sperm DNA, denatured; 5x Denhardt's solution
Protease inhibitor cocktail (50x)	1 Complete protease inhibitor tablet (Roche) dissolved in 1ml water
Restriction enzyme buffers (10x)	MBI Fermentas, St. Leon-Rot, Germany
RIPA buffer	50mM TrisHcl pH 7.4; 150mM NaCl; 1% NP-40; 0,5% sodium deoxycholate; 0,1% SDS; 5mM EDTA; 1xProtease inhibitor cocktail
SDS PAGE sample buffer (3x)	0.15M Tris/HCl, pH 6.8; 6% SDS; 30% (w/v) glycerol; 0.003% Bromphenol Blue; 75mM DTT
Separating buffer (Western) (4x)	1.5M Tris/HCl pH 8.8; 0.4% SDS
SSC (20x)	3M NaCl; 0.3M sodium citrate, pH 7.0
Stacking buffer (Western) (4x)	0.5M Tris/HCl pH 6.8; 0.4% SDS
Stripping solution (Southern)	0.5% SDS
Stripping solution (Western)	50mM Tris, 2% SDS, 100mM 2-mercaptoethanol, pH 6.8
TAE-buffer (50x)	2M Tris; 57% acetic acid; 100mM EDTA; pH 8.0
Taq-Polymerase Puffer (10x)	MBI Fermentas
TBS (Tris buffered saline) (10x)	0.5M Tris base, 9% NaCl, pH 7.6

TBS/T buffer	1x TBS buffer, 0.1% Tween
TE-buffer	10mM Tris/HCl, pH 7.5; 1mM EDTA
Transfer buffer (Southern)	0.4N sodium hydroxide
Transfer buffer 5x (Western)	200mM glycine; 250mM Tris; 0.185% SDS; pH 8.3
Transfer buffer 1x (Western)	1:1:3 (v/v) 5x transfer buffer:methanol:water
Washing solution I (Southern)	2x SSC, 0.2%SDS
Washing solution II (Southern)	0.2xSSC, 0.2%SDS

3.3 Filters and membranes

Cell strainer, 40μm nylon; BD Biosciences

Whatman 3MM chromatography paper; Satorius

Nylon membrane (Southern); Biodyne®B, 0.45μm PALL Gelman Laboratory, USA

Nitrocellulose membrane (Western); porablot NCP, Macherey-Nagel, Germany

PVDF membrane (Western); porablot PVDF, Macherey-Nagel, Germany

3.4 Antibodies

3.4.1 Antibodies used for Fluorescence Activated Cell Sorting (FACS)

Antigen	*Fluorochrome*	*Producer*
Annexin V	APC, FITC	BD Biosciences PharMingen, San Diego, USA
B220 (RA3-6B2)	APC	BD Biosciences PharMingen
CD3ϵ (145-2C11)	biotin, APC	BD Biosciences PharMingen
CD3ζ (H146-968)	PE	EuroBioSciences

CD4 (L3T4)	FITC,PE,APC	BD Biosciences PharMingen
CD5 (53-7.3)	biotin	BD Biosciences PharMingen
CD8a (53-6.7)	FITC,PE	BD Biosciences PharMingen
CD24 (HSA, M1/69)	PE	BD Biosciences PharMingen
CD25 (PC61)	APC	BD Biosciences PharMingen
CD25	FITC	Southern Biotechnology Associates, USA
CD44	biotin	BD Biosciences PharMingen
CD45RB	FITC	BD Biosciences PharMingen
CD62L (MEL-14)	PE	BD Biosciences PharMingen
CD69 (H1.2F3)	PE	BD Biosciences PharMingen
TCRβ (H57-597)	biotin, PE	BD Biosciences PharMingen
TCR$\gamma\delta$ (GL3)	PE	BD Biosciences PharMingen

For detection of biotinylated antibodies by FACS, streptavidin coupled with FITC, PE or APC was used (BD Biosciences Pharmingen).

3.4.2 Antibodies used for thymocyte stimulation

Purified NA/LE Hamster Anti-mouse CD3e (145-2C11); BD Biosciences PharMingen

Purified NA/LE Hamster Anti-mouse CD28 (37.51); BD Biosciences PharMingen

Purified anti-Armenian and Syria Hamster IgG (G192-1); BD Biosciences PharMingen

3.4.3 Antibodies used for Western Blotting

Antigen	*Host*	*Producer*
Actin (I-19)	Goat	Santa Cruz Biotechnology, Inc.
c-Cbl (C-15)	Rabbit	Santa Cruz Biotechnology, Inc.
Cbl-b	Rabbit	Santa Cruz Biotechnology, Inc.
c-Fos (H125)	Rabbit	Santa Cruz Biotechnology, Inc.
ERK1 (MK1)	Mouse	BD Biosciences Pharmingen

Fyn	Rabbit	Santa Cruz Biotechnology, Inc.
Gads	Rabbit	Upstate, USA
GRAIL (H11-744)	Rat	Pharmingen
Grb2 (C-7)	Mouse	Santa Cruz Biotechnology, Inc.
Hrs	Rabbit	Raiborg *et al.*, EMBO J 20, 5800, 2001
Itch	Mouse	BD Biosciences
LAT	Rabbit	Cell Signaling Technology, Inc.
Lck	Mouse	Santa Cruz Biotechnology, Inc.
Phospho-ERK1/2 (Thr202/Tyr204,	Rabbit	Cell Signaling Technology, Inc.
Phospho-LAT (Tyr191)	Rabbit	Cell Signaling Technology, Inc.
Phospho-Tyr (4G10)	Mouse	AG Schraven
Phospho-Zap70 (Tyr319/Syk(Tyr352))	Rabbit	Cell Signaling Technology, Inc.
SLP-76	Goat	Santa Cruz Biotechnology, Inc.
STAM2	Rabbit	Bache *et al.*, J Biol Chem 278, 12513, 2003
Ubiquitin (FL-76)	Rabbit	Santa Cruz Biotechnology, Inc.
UBPY (31aa)	Rabbit	University of Oxford, Institute of Molecular Medicine
Zap70 (99F2)	Rabbit	Cell Signaling Technology, Inc.

Secondary antibodies from donkey against goat, mouse, rabbit and rat coupled to horseradish peroxidase (HRP) were from Santa Cruz Biotechnology, Inc.

3.5 Recombinant cytokines and proteins

Interleukin-2 from mouse, recombinant expressed in E.coli; Sigma-Aldrich, USA

3.6 Enzymes

NcoI; MBI Fermentas

Proteinase K(10mg/ml); PAN Biotech GmbH

Taq DNA Polymerase; MBI Fermentas

3.7 Kits

murine IL-2 ELISA Ready-SET-Go!	eBioscience
NucleoSpin™ExtractII kit	Macherey-Nagel, Düren, Germany
QIAexII™Gel extraction kit	Qiagen, Hilden, Germany
Rediprime™II	Amersham Biosciences, Munich, Germany
APC BrdU Flow Kit	BD Pharmingen

3.8 Primers used for Southern Blot probe

sense GGT AGC ACG GAG AGT AAT TT

antisense CCG GGT TGC CAG AAT TAG GT

3.9 Cell culture media

3.9.1 Basic components and supplements

RPMI 1640	PAA Laboratories, Pasching, Germany
Fetal calf serum (FCS, heat inactivated 30 min on 56°C)	Biochrom, Berlin, Germany

L-Glutamine	Cambrex, Verviers, Belgium
Penicillin/Streptamycin	Cambrex, Verviers, Belgium

3.9.2 Media

Complete T cell medium	RPMI, 10%FCS, 0.2mM glutamine, 100U/ml penicillin, 100μg/ml streptomycin
Starving medium	RPMI, 100U/ml penicillin, 100μg/ml streptomycin
Stimulation medium	RPMI, 100U/ml penicillin, 100μg/ml streptomycin, 10μg/ml anti-CD3e, 2μg anti-CD28, 10μg anti-hamster antibodies

3.10 Equipment

Automated cell counter	CASY Scharfe System, Reutlingen, Germany
ELISA reader	Tecan, Kreisheim, Germany
Flow cytometer FACSCalibur, with CellQuest software	BD Biosciences, Heidelberg, Germany
GenAmp®PCR System 9700	Perkin Elmer, Wellesley, USA
Mastercycler®Gradient	Eppendorf, Hamburg, Germany
Mini-gel system for vertical electrophoresis (PAGE)	Bio Rad, USA
Chambers for horizontal electrophoresis	Bio Rad, USA
TransBlot SD Semidry Transfer cell	Bio Rad, USA
IMAGE Reader	Fujifilm, Düsseldorf, Germany
Phosphoimager	Amersham Bioscience, Buckinghamshire, UK
UV Stratalinker® 2400	Stratagene, CA, USA
Photometer	Eppendorf, Hamburg, Germany
Gased incubator	Heraeus, Hanau, Germany
Laminar flow benches	Heraeus, Hanau, Germany
Scintillation counter	Wallac, Turcu, Finland

Centrifuges	Beckman Coulter, Krefeld, Germany; Eppendorf, Hamburg, Germany; Hettich, Tuttlingen, Germany

3.11 Mice

UBPY$^{flox/flox}$-deficient mice (on C57/BL6 - 129/Ola mixed background) were generated as described [9].

CD4cre mice (on C57/BL6 - 129/Ola mixed background) were provided by Chris Wilson, University of Washington.

All experiments described in this work were performed with 4-12 weeks old mice housed under specific pathogen-free conditions in accordance with the German animal protection law.

Chapter 4

Methods

4.1 DNA and RNA Methods

4.1.1 Phenol Chloroform extraction

The phenol/chloroform extraction is used to separate proteins and nucleic acids and to remove salts by the subsequent precipitation by isopropanol. A DNA solution was transferred to Phase-Lock-tubes (Eppendorf). 500μl of a Phenol/Chloroform/Isoamylalcohol solution (25:24:1) were added to the tube and mixed vigourously. Phases were separated by centrifugation for 5 minutes at 20.000xg. Then 500μl of a Chloroform/Isoamylalcohol solution (24:1) were added and again mixed vigourously. The tubes were again centrifuged for 5 minutes at 20.000xg. The acqueous phase containing the extracted DNA could then be further processed.

4.1.2 DNA precipitation

For DNA precipitation, a DNA solution was carefully mixed with an equal volume of isopropanol. The DNA was then pelleted by centrifugation for 15 minutes at 20.000xg. The su-

pernatant was discarded, the DNA pellet washed with 70% Ethanol and air-dried. The DNA was then resuspended in water or TE buffer for further processing.

4.1.3 Isolation of genomic DNA from cells and organs

Pelleted cells, tissues (≈20mg) or mouse tails (≈10mm) were resuspended in 700μl DNA lysis buffer (680μl TENS buffer supplemented with 60μg/ml proteinase K) and incubated over night at 56°C until complete dissolution of the tissue. Subsequently the DNA was isolated using the Phase-lock-tubes (Eppendorf). The DNA was precipitated, resuspended in 150μl TE buffer and dissolved overnight at 56°C.

4.1.4 Determination of DNA concentration by photospectrometry

This method can be applied to concentrations above 50μg/ml of nucleid acids. In a photometer the absorption at 260 and 280nm of the diluted sample (1/20 to 1/200) is measured using the solvent as reference. In case of doublestranded DNA, $OD_{260} = 1$ corresponds to a concentration of 50μg/ml. In case of single stranded RNA or DNA $OD_{260} = 1$ corresponds to a concentration of 40μg/ml. Purity of the probe is given by the quotient OD_{260}/OD_{280}, with optimal values being 1.8 for DNA probes and 2.0 for RNA probes.

4.1.5 Digestion of DNA with restriction enzymes

50μg of genomic DNA were incubated overnight with 1 unit/μg of restriction enzyme at the conditions indicated by the manifacturer.

4.1.6 Electrophoretic separation of DNA fragments

For the electrophoretic separation of DNA fragments, 1% agarose gels were used. The gels were prepared by boiling the agarose in 1xTAE-buffer in the microwave oven, and then cooling to approximately 60°C. For the visualization of DNA fragments, ethidium bromide is added in final concentration of 10ng/ml. The mixture is poured in horizontal casting chambers and allowed to polymerize. The samples are prepared for loading by mixing with 0.1 volume 10x loading buffer. The fragment separation is performed in TAE buffer, under 70-100V.

4.1.7 Extraction of DNA fragments from agarose gels

The DNA bands were visualized by exposure to UV light and the desired fragment excised. The gel fragment was transferred to an Eppendorf tube. Extraction of the DNA was performed using the QIAexII® Gel Extraction Kit (Qiagen) according to the manufacturer's instructions.

4.1.8 Polymerase chain reaction (PCR)

The standard PCR reaction mix was composed as follows:
0,5μM sense primer
0,5μM antisense primer
1x Taq polymerase buffer
1,5mM $MgCl_2$
200μM dNTP-Mix
2,5U Taq polymerase
5-100ng DNA template
The volume was adjusted to 25μl with water.
For amplification of the Southern probe, the PCR was carried out in a thermocycler with the following program:

REACTION STEP	CYCLES	TEMPERATURE	DURATION
Initial denaturation	1	95°C	1min
Denaturation		95°C	50sec
Annealing	15	60°C	50sec
Elongation		72°C	3min
Final elongation	1	72°C	7min

4.1.9 Southern Blot

Blotting of the DNA

The digested genomic DNA was separated on a 0.7% agarose gel at 70V. The DNA was visualized by exposure to UV light and photographed together with a ruler, allowing size assignment of detected fragments. The Southern Blot was assembled as follows (from bottom to top): three layers of Whatman paper with their ends soaking in a buffer reservoir filled with transfer solution (0.4N Sodium hydroxide), the gel, the nylon membrane (adjusted to gel size), three layers of whatman paper, a stack of paper towels, a glass plate and a weight on the glass plate. The capillary transfer was performed at room temperature for 15 to 24 hours. The membrane was rinsed with 2xSSC to remove the sodium hydroxide and used for hybridization with the Southern probe.

Preparation of the radioactively labeled probe

The specific probes were made by PCR amplification (as described in Section 4.1.8) with the primers listed in Section 3.8 using genomic DNA from wild type mouse embryonic fibroblasts as template. The amplified fragments were purified by NucleoSpinR ExtractII kit (Macherey-Nagel, Duren, Germany) according to the manufacturers instruction. For the radioactive labeling of the probe, the kit Rediprime®II (Amersham Biosciences) was used according to the manufacturers instruction. Shortly, 2-20ng of the probe were diluted with TE buffer up to 45μl,

denatured for 5 minutes on 95°C and cooled on ice for 5 minutes. The denatured probe was added to the Rediprime-mix together with 5μl of [α-32P]dCTP and incubated 30 minutes on 37°C. During this step, the enzyme Klenow-polymerase synthesizes the second cDNA strand using the randome priming principle and builds in the radioactive dCTPs in the nucleotide strands. The unbound radioactive dCTPs are removed by another purification step with the NucleoSpinR ExtractII kit. The purified radioactive probe was denatured again on 95°C, cooled on ice for 5 minutes and used immediately for hybridization.

Hybridization, washing and exposure

The pre-hybridization (blocking) of the membrane was performed in 5ml of pre-hybridization solution (5x SSC; 0,5% SDS; 100μg/ml denatured salmon sperm DNA; 5x Denhardt's solution) on 63°C for 6 hours. After the pre-hybridization, the radioactively labeled, purified and denatured probe was added to the solution and incubation was continued on 63°C overnight. In order to remove the unspecifically bound radioactive probe, the membrane was washed first with the Wash solution I for 20 minutes on 55°C (low stringency wash buffer) and then two more times with the Wash solution II (higher stringency wash buffer), each time 20 minutes on 55°C. Washed membrane was placed on the phosphoimager screen and exposed overnight. Finally, the screen was scanned with the Phosphoimager.

Stripping and reprobing

In order to prepare the membrane for the new hybridization, the membrane was 'stripped' with boiling 0.5% SDS solution. The hybridization procedure was repeated with the new probe in the same way as described above, starting with the pre-hybridization step.

4.2 Histology

4.2.1 Preparation of tissue sections

For fixation, tissues were removed, washed if necessary in ice-cold PBS and incubated overnight in acid formalin and stored in 10% buffered formalin. Water from the tissues was removed by serial incubation steps with ascending concentrations of ethanol and the tissues embedded in paraffin. From the paraffin blocks, 4μm sections were cut, stretched at 37°C and attached to coated microscope slides. Before staining, the tissue sections were deparaffinized by incubating two times for five minutes in xylol, after which the sections were rehydrated to 30% ethanol. Finally the slides were washed in water and incubated in PBS for five minutes.

4.2.2 Eosin/Hematoxylin staining

Eosin/hematoxylin staining was performed according to standard protocols.

4.2.3 Immunohistochemistry

For immunostaining, 4μm thick sections of formalin-fixed, paraffin-embedded tissue was cut, deparaffinized, and subjected to a heat induced epitope retrieval step. The slides were rinsed in cool running water and washed in Tris-buffered saline (pH 7.4) before incubation with primary antibodies against CD3 (#N1580, Dako, Glostrup, Denmark, dilution 1:10) and Foxp3 (FJK-16s, eBioscience, 1:100) for 30 minutes. For detection biotinylated donkey anti-rat or donkey anti-rabbit (Dianova, Hamburg, Germany) secondary antibodies were used followed by the streptavidin-AP kit (K5005, Dako) or the EnVision peroxidase kit (K 4010, Dako). Alkaline phosphatase was revealed by Fast Red as chromogen and Peroxidase was developed with a highly sensitive diaminobenzidine (DAB) chromogenic substrate for approximately 10 minutes.

Negative controls were performed by omitting the primary antibodies. (Histology was performed by Prof.Dr.Christoph Loddenkemper, Charité Berlin)

4.3 Protein methods

4.3.1 Preparation of RIPA protein extracts

The total protein extracts from cells were obtained by lysis in the RIPA buffer supplemented with a protease inhibitor cocktail (Roche). The amount of the lysis buffer was adjusted to contain 5x10^5 cells/μl. Cells were pelleted by centrifugation for 5 minutes at 560xg and resuspended in a small drop of PBS (approximately the size of the cell pellet). The cells were incubated in the lysis buffer on ice for 30 minutes and then centrifuged for 30 minutes on 20.000xg on 4°C. Clarified lysates were transferred into fresh tubes and the protein concentration was determined by Bradford method (Section 4.3.2). The proteins were denatured by adding 1/2 volume of the 3xSDS PAGE sample buffer and boiled for 5 minutes on 95°C. After denaturing, the samples were cooled on ice, briefly centrifuged and used immediately for electrophoresis or frozen on -20°C.

4.3.2 Protein concentration determination (Bradford assay)

For determination of protein concentrations in protein extracts, the 5x Roti®-Nanoquant solution (Roth) was used. BSA standard dilutions in a range from 1 to 50μg/ml were prepared with a total volume of 200μl. For the zero value of the standard curve, 200μl of water were used. The protein samples were appropriately diluted (usually 1:10 to 1:50 with the RIPA extracts prepared as described in section 4.3.1) in water in a total volume of 200μl. The protein standards and the diluted samples were pipetted in polystyrene cuvettes. The 5x Nanoquant solution was diluted 1:5 with

water, 800μl of this working solution added to each cuvette and carefully mixed by inverting the cuvettes several times. The OD_{595} of each sample was measured in a spectrophotometer using pure water as reference. The OD_{595} of the standards were used to establish a standard curve which was then used to determine the protein concentrations of the samples.

4.3.3 SDS polyacrylamide gel electrophoresis (SDS-Page)

The proteins were separated by size on vertical polyacrylamide gels in an electophoresis chamber (Bio-Rad) filled with electrophoresis buffer. The gels consisted of a low-percentage stacking gel (pH 6.8) on top of a separation gel (pH 8.8). The composition of the gels are indicated in the tables below. Proteins loaded onto the gel were denatured by prior heat-treatment in SDS-PAGE sample buffer. β-Mercaptoethanol in the sample buffer reduces disulphide bonds in proteins and negatively charged SDS associates with hydrophobic residues of the proteins. The stacking gel ensures simultaneous entry of proteins of all sizes into the separation gel. The negatively charged proteins are then separated in the electric field proportional to the logarithm of their mass.

SEPARATING GEL	Final acrylamide concentration in separating gel (%)							
Stock solutions	5	7,5	8	9	10	12	15	20
30%acrylamide/ 0,8% bisacrylamide (ml)	2,5	3,75	4	4,5	5	6	7,5	10
4xTris.Cl/SDS pH 8.8 (ml)	3,75	3,75	3,75	3,75	3,75	3,75	3,75	3,75
H_2O (ml)	8,75	7,5	7,25	6,75	6,25	5,25	3,75	1,25
10% APS (μl)	50	50	50	50	50	50	50	50
TEMED (μl)	10	10	10	10	10	10	10	10

STACKING GEL Stock solutions	
30%acrylamide/ 0,8% bisacrylamide (ml)	0,65
4xTris.Cl/SDS pH 6.8 (ml)	1,25
H_2O (ml)	3,05
10% APS (μl)	36
TEMED (μl)	6

4.3.4 Detection of Proteins immobilised on membranes with antibodies (Western Blot)

The polyacrylamide gel was removed from the electrophoresis chamber and cut on the glass plate to an appropriate size. Proteins were transferred from the gel onto a nylon membrane (PVDF membranes were used for very small proteins <30kDa) by semi-dry blotting (TransBlot SD Semi-Dry Transfer Cell, Bio Rad). Six layers of Whatman 3MM chromatography paper were soaked in transfer buffer and placed onto the anode. The nylon membrane (prewetted in transfer buffer) or the PVDF membrane (prewetted in 100% methanol) and the gel slice were positioned on top of the filter paper. Finally six further layers of Whatman paper soaked in transfer buffer were applied. Air bubbles were removed after each step. A constant voltage of 20 V for 1 hour transferred the proteins. Before blocking, successful and homogeneous transfer of the proteins to the membrane was tested by Ponceau S staining. The membrane was incubated for 5 minutes at room temperature in Ponceau S solution. After that the membrane was washed with TBS-T until distinct bands were visible. Optionally a picture of the Ponceau S stained membrane was taken. The membrane was then incubated in blocking buffer appropriate for the individual antibody and remained in the solution for at least 1 hour at room temperature to saturate non-specific binding sites on the membrane. The membrane was incubated with the primary detection antibody overnight at 4 °C on a nutator. After washing three times for 10 min in TBST, the secondary HRP-coupled antibody in blocking solution (1:3000) was added and incubated for 1 h. After a second washing step with three times TBST for 10 min, the freshly mixed ECL detection solutions (Immobilon^{TM}Western) were applied for at least 1 min. Excess liquid from the membrane was drained with filter papers. Light produced by catalytic oxidation of luminol in the detection solution through the horse radish peroxidase was detected with the Image Reader (Fujifilm).

4.3.5 Stripping

Blots were incubated 2x 20 min at 50 °C in pre-warmed blot stripping buffer, with gentle shaking. Afterwards, the membrane was rinsed 3x 5 min in TBS, then reblocked.

4.3.6 Preparation of protein extracts from stimulated thymocytes

Thymocyte single cell suspensions and lysis of erythrocytes was carried out as described in 4.4.1. The cell suspensions were then adjusted to a cell concentration of 4.10^7cells/ml in starving T cell medium. For each timepoint, 4.10^6cells were used. For starvation, the cells were incubated for 15 minutes at 37°C. After that, the cells were pelleted and incubated in stimulating medium (complete T cell medium supplemented with 10μg/ml CD3ϵ antibody, 10μg/ml Hamster IgG antibody, 2μg/ml CD28 antibody) at 37°C with gentle rocking (200rpm). At each timepoint a 100μl sample of the stimulated cell suspension was taken and transferred in an eppendorf tube with 50μl of boiling 3xSDS sample buffer and incubated for 15 minutes at 95°C with vigourous shaking (1000rpm). The resulting SDS buffer protein samples were stored at -20°C until used for Western Blotting.

4.4 Cell biological methods

4.4.1 Preparation of single-cell suspensions of primary cells

Isolation of primary cells

After sacrificing the mice by CO_2 inhalation, organs (spleen, lymph nodes, thymus) were removed, shortly washed with PBS and placed in PBS on ice. Single-cell suspension from organs were obtained by pressing small pieces of the isolated organs with the tampon of a syringe

through a 40μm nylon cell strainer in a petri-dish with cold PBS. The cell strainer was then transferred onto a 50ml Falcon tube and the PBS with the cells pipetted through the cell strainer in the tube. Remaining cells on the petridish were collected by rinsing once with PBS and also pipetted in the tube through the cell strainer. Cells were further resuspended by careful pipeting several times. Single cell suspensions were stored on ice until further processing.

Lysis of erythrocytes

For lysis of erythrocytes, cells were pelleted by centrifugation for 15min at 600xg. The cell pellet was then resuspended in 1x PharmLyse^{TM}buffer (BD Biosciences) and incubated for 7 minutes at room temperature. 4ml of buffer were used for one spleen and 2ml for one thymus. Then the reaction was stopped by addition of 12ml of PBS and the cells pelleted again. The cell pellet was then resuspended in PBS or medium and stored on ice.

4.4.2 Fluorescence Activated Cell Sorting (FACS)

Cell samples of 0.5-1x10^6 cells were resuspended in 100μl FACS buffer with 0.5μl of desired fluorchrome-coupled or biotinylated antibodies (maximum of 3 different fluorochromes was used) and incubated for 20 minutes on room temperature, protected from light or, when indicated, for one hour at 4°C. After incubation, excess antibody was removed by washing the cells two times with FACS buffer. In case biotinylated antibodies were used, streptavidin coupled with fluorochrome was used in the second staining step (0.5μl of fluorochrome coupled streptavidine in 100μl FACS buffer) and incubated 20 minutes on room temperature, protected from light, or, when indicated, for one hour at 4°C. After labeling, cells were washed once, resuspended in 150μl FACS buffer and analyzed.

4.4.3 *In vivo* BrdU labeling

Mice 4 weeks of age were killed 2 h after intraperitoneal injection with 100 ml of a 10mg/ml solution of BrdU. BrdU incorporation in thymocyte subsets was analyzed with the BD Pharmingen BrdU Flow Kit according to the manufacturer's instructions.

4.4.4 Survival assay

Thymocyte single cell suspension were prepared and erythrocytes lysed as described in 4.4.1. The cells were resuspended in starving medium at a concentration of 4.10^6cells/ml. 100μl of this cell suspension was added per well of a 96-well plate and the plate incubated at 37°C. After 0, 24 and 48 hours the cells were transferred to FACS tubes, pelleted and resuspended in 1x Annexin staining buffer with 2.5μl AnnexinV-APC and 2.5μl Propidium iodide (PI). Staining was carried out for 20 minutes at room temperature. After that further 150μl of 1x AnnexinV staining buffer were added and the cells acquired by Flow Cytometry. Viable cells were determined as AnnexinV negative cells within the Propidium iodide-negative gate and expressed as percentage of the viable cells at $t = 0h$.

4.4.5 Proliferation assay

A 96well round bottom plate was coated with 30μl per well of CD3ϵ antibody dilutions in PBS (at the following concentrations: 0.1; 1; 10; 50 μg/ml) for 2 hours at 37°C. After this incubation the plates were washed three times with 200μl PBS per well. Thymocyte single-cell suspensions were prepared and erythrocytes lysed as described in 4.4.1. The concentration of the cell suspensions was adjusted to 10^6cells/ml in complete T cell medium. 200μl of the cell suspensions were added per well and incubated at 37°C for 96 hours. For additional interleukin-2 stimulation, recombinant mouse Interleukin-2 (Sigma-Aldrich) was added at a final concentration of 100u/ml

to the medium. During the last twenty hours, cells were pulsed with 1μCi ^{3}H-thymidine (GE Healthcare) per well. After the incubation period, cells were harvested on filtermats (Wallac) using a semi-automated cell harvesting apparatus (Inotech). The filtermats were dried, coated with Melt-on scintillation sheets (Wallac) and counted in a scintillation counter (Wallac).

4.4.6 Interleukin-2 ELISA

For detection of Interleukin-2 in cell culture supernatants of stimulated thymocytes we used the mouse Interleukin-2 ELISA-Ready-SET-Go! Kit (eBioscience).

Coating

First the ELISA plates are coated with 100μl per well of a dilution of the capture antibody in coating buffer (48μl capture antibody in 12 ml coating buffer), sealed and incubated overnight at 4°C. The coated plates can be stored for maximum one week at 4°C.

Blocking

The next day the coated plates are washed five times: the wells were aspirated, 250μl wash buffer per well were added and let 1 minute to soak, then the wash buffer was aspirated and the plates were blotted on absorbent paper to remove residual wash buffer. This was repeated five times. Then the plates were blocked by incubating the well with 200μl Assay diluent for one hour at room temperature. Plates were covered during each incubation step. After blocking, the plates were washed five times as previously described.

Preparation of standards

Using assay diluent, serial dilutions of a Interleukin-2 standard were prepared. Dilution of 4μl standard in 20ml assay diluent gave the top standard dilution (200pg/ml). Starting with the top standard dilution, 2-fold serial dilutions were performed to make the standard curve (range 2-200pg/ml).

Capture

100μl of the standards and 100μl of the samples to be tested were added in triplicates to the appropriate wells and incubated at room temperature for 2h (or overnight at 4°C in a sealed plate for maximal sensitivity) Then the plates were washed five times as previously described.

Detection

100μl of the detection antibody were added per well and incubated for one hour at room temperature. The plates were washed again five times. 100μl of the enzyme solution were added to each well and incubated for 30 minutes at room temperature. The plates were washed seven times. 100μl of substrate solution were added to each well and incubated for 15 minutes at room temperature. The reaction was stopped by adding 50μl of the stop solution to each well and the plates were read at 450nm in an ELISA plate reader.

4.4.7 *In vitro* induction of apoptosis

A 96-well round bottom tissue culture plate was coated overnight with antibodies against CD3ϵ and CD28 (50μg/ml each) at 4°C. The next day, the plate was washed three times with PBS and 100μl of a thymocyte single cell suspension (4.10^{6}cells/ml) in complete T cell medium prepared as described in section 4.4.1 added per well. The plates were incubated overnight at

37°C. The next day, the cells were resupended in 100μl 1xAnnexin staining buffer with 2,5μl AnnexinV-APC and 2,5μl Propidium iodide (PI) and staining was performed for 20 minutes at room temperature. Then 150μl 1x Annexin staining buffer were added to the samples and the samples acquired by Flow Cytometry. Viable cells were determined by negative staining for both the Apoptosis marker Annexin V and the vital dye Propidium iodide. Cells in early apoptosis are positive for AnnexinV, but still negative for PI staining. Cells in late apoptosis, as well as necrotic cells are positive for both stains.

4.4.8 Detection of ligand induced surface TCR downmodulation

Thymi were removed and single-cell suspensions prepared as described in section 4.4.1. After lysis of the erythrocytes, the cells were counted using the Casy® cell counter and the cell concentration adjusted to 4.10^6 cells/ml in ice-cold complete T cell medium. For each timepoint 1.10^6 cells were used and transferred to FACS tubes. First, the cells were stained for 30 minutes at 4°C with 3μl biotinylated TCRβ antibody. To start the stimulation, cells were pelleted by centrifugation for 5 minutes at 560xg at 4°C and resuspended in 250μl complete T cell medium supplemented with 1,5μl anti-hamster IgG prewarmed to 37°C. The resuspended cells were then incubated at 37°C for the desired times. After the desired incubation time, 250μl of ice-cold PBS were added to the tubes, to stop the reaction and the tubes stored on ice. When all samples were collected, the cells were pelleted again by centrifugation for 5 minutes at 560xg at 4°C and stained in 100μl FACS buffer with CD4-APC, CD8α-FITC and streptavidin-PE (0.5μl each) for 30 minutes at 4°C. Since the cells were not permeabilized previous to the staining, streptavidin-PE binds only to the TCR-biotinlyated antibody complexes remaining at the surface. The levels of surface TCR at t were expressed as percentage of the surface TCR present at $t = 0$ ($\%SF_0$), using the median fluorescence intensity (MFI) of PE in the CD4SP or DP gates with the follow-

ing formula: $\%SF_0 = (100 * MFI_t)/(MFI_0)$ with MFI_t being the MFI at a timepoint and MFI_0 being the MFI of cells before stimulation.

4.4.9 Ligand independent regulation of TCR surface levels

Thymi were removed and single-cell suspensions prepared as described in section 4.4.1. After lysis of the erythrocytes, the cells were counted using the Casy® cell counter and the cell concentration adjusted to 4.10^6 cells/ml in ice-cold complete T cell medium. For each timepoint 1.10^6 cells were used and transferred to FACS tubes. To start the measurement, cells were pelleted by centrifugation for 5 minutes at 560xg at 4°C and resuspended in 250μl complete T cell medium alone or supplemented with 10μg/ml Brefeldin A or supplemented with 50μg/ml cycloheximide prewarmed to 37°C. The resuspended cells were then incubated at 37°C for the desired times. After the desired incubation time, 250μl of ice-cold PBS were added to the tubes, to stop the reaction and the tubes stored on ice. When all samples were collected, the cells were pelleted again by centrifugation for 5 minutes at 560xg at 4°C and stained in 100μl FACS buffer with CD4-APC, CD8α-FITC and TCRβ-PE (0.5μl each) for 30 minutes at 4°C. Since the cells were not permeabilized previous to the staining, TCRβ-PE binds only to the TCR remaining at the surface. The levels of surface TCR at t were expressed as percentage of the surface TCR present at t ($\%SF_0$) in untreated cells, using the median fluorescence intensity (MFI) of PE in the CD4SP or DP gates with the following formula: $\%SF_0 = (100 * MFI_{tr}(t))/(MFI_{untr}(t))$ with $MFI_{treated}(t)$ being the MFI of the treated cells at a timepoint and $(MFI_{untr}(t)$ being the MFI of untreated cells at the same timepoint.

Chapter 5

Results

5.1 Generation of mice with a T cell specific UBPY knockout (UBPY$\triangle^T$)

The conventional knockout of UBPY causes embryonic lethality and the induced global knockout in mature animals leads to the death of the animals within seven days [9], thus making these mouse models unsuitable for the study of T cell specific functions of UBPY. Therefore a T cell-specific UBPY gene knockout mouse was generated using the cre/LoxP system. This is a naturally occurring site specific recombination system derived from the bacteriophage P1. The cre recombinase mediates site-specific recombination between two sequences of 34bp, called LoxP sites. A loxP site (locus of X-ing over) consists of two 13 bp inverted repeats separated by an 8 bp asymmetric spacer region conferring directionality to the site. Two LoxP sites in direct orientation on a DNA molecule dictate excision of the intervening DNA between the sites leaving one LoxP site behind. Previous work in our lab used gene targeting to create mice with exon 4 of the UBPY gene flanked by two LoxP sequence motifs (UBPY $^{flox/flox}$) [9]. Cre-mediated

deletion of exon 4 causes a shift in the reading frame and introduces several stop codons in the RNA. This RNA may produce a severely truncated protein of only 88 amino acids, lacking all functional domains, including the catalytic region and the diverse protein binding domains (see Fig.1.6) However, it is likely that this truncated protein is instable and rapidly degraded.

The UBPY $^{flox/flox}$ were bred with mice expressing the *cre* transgene under the control of the *cd4* promoter. In the thymus, maturation of thymocytes proceeds through three stages classified according to expression of the surface markers CD4 and CD8. The earliest stage is the double-negative (DN) stage, in which neither of both coreceptors is expressed. The DN stage is further subdivided in four stages according to expression of the surface markers CD44 and CD25 (DN1-DN4). Thymocytes having successfully rearranged the T cell receptor beta chain (TCRβ) during DN3 are selected, expand and proceed to the double-positive stage. DP thymocytes rearrange the TCR α chain and undergo a second round of selection based on the specificity of the mature TCR heterodimer for self-antigen associated to molecules of the major histocompatibility complex. As a result of this process, a relatively small fraction of DP thymocytes mature to either CD4+ or CD8+ single positive (SP) cells and finally emigrate to peripheral lymphoid organs as naïve T cells. Since CD4 expression is initiated after successful rearrangement of the TCRβ during DN3, the expression of the cre recombinase also starts at that time. Therefore in UBPY $^{flox/flox}$/CD4 cre$^+$ mice, UBPY deletion begins at the DN4 stage and should be completed in the double-positive thymocytes, single positive CD4+ and CD8+ single positive thymocytes and the peripheral CD4+ and CD8+ T cells.

The UBPY deletion was tested with a Southern probe recognizing a 5kb NcoI fragment in wild-type DNA. After cre mediated recombination the fragment recognized by the probe is 6kb long, due to the excision of a NcoI restriction site (Fig.5.1A). The majority of double negative thymocytes still carry the floxed *UBPY* allele. This is in accordance with the expectations, since cre expression under the *cd4* promoter only starts at double negative stage 3. The highest deletion

rate is achieved in double positive thymocytes, with nearly 80% of the cells bearing the *UBPY*Δ allele. Higher levels of the nonrecombined *UBPY* allele were detected in FACS-sorted peripheral T cells from spleen and mesenterial lymph nodes, indicating the presence of T cells derived from thymocytes with an incomplete deletion of UBPY. In accordance to the results of the Southern Blot, immunoblot analysis of protein extracts from total thymocytes revealed the presence of a fraction of UBPY expressing cells, with the majority probably being double-negative thymocytes. Indeed, in sorted DP thymocytes the fraction of cells still expressing UBPY is so small, that UBPY expression is below detection level.

These results show that UBPY $^{flox/flox}$/CD4 cre^{+} mice yield at least in part UBPY depleted DP and SP thymocytes, as well as peripheral CD4+ and CD8+ T lymphocytes, representing therefore a convenient tool for the study of the role of UBPY in T cells. Subsequently UBPY $^{flox/flox}$/CD4 cre^{+} mice will be referred to as UBPYΔ^T

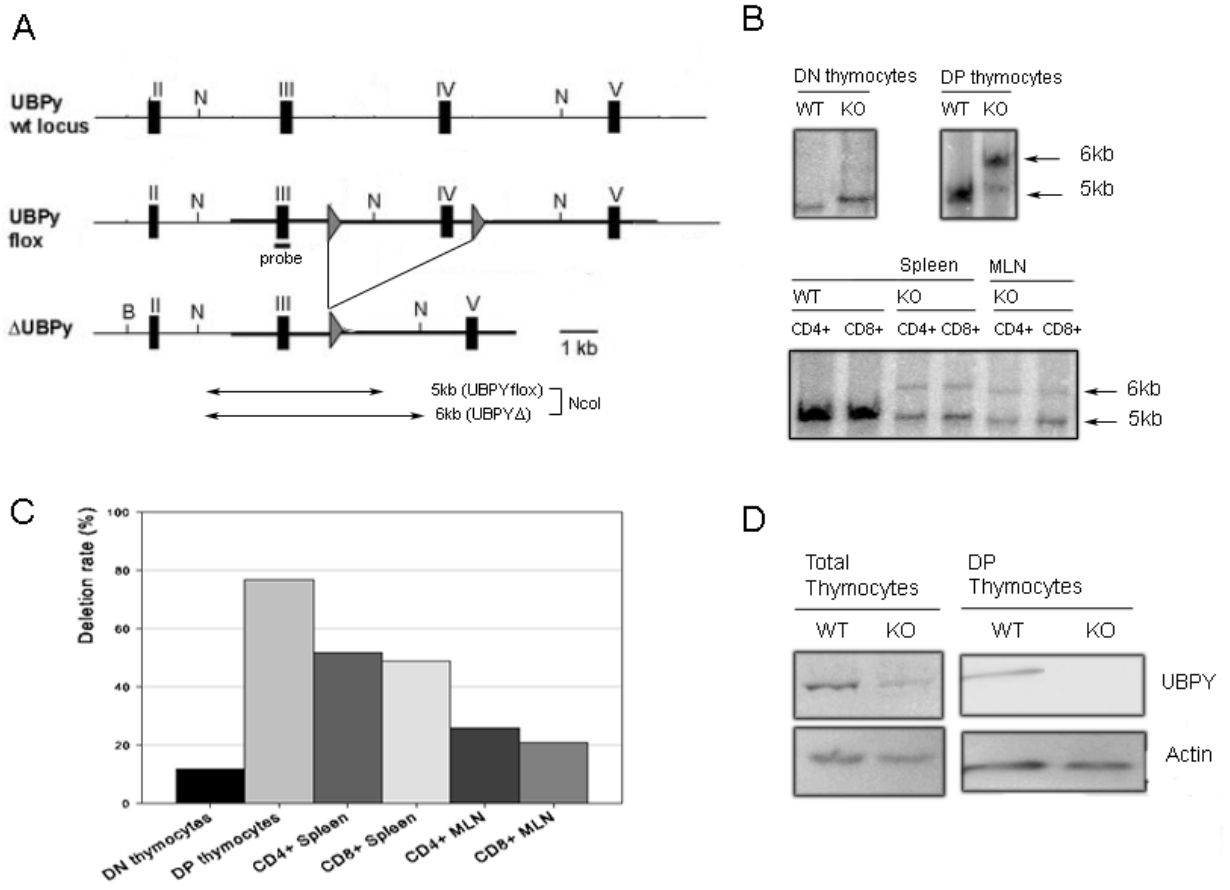

Figure 5.1: Generation of UBPYΔ^T mice. (A) Diagram showing the wildtype *Ubpy* genomic locus, the loxP-flanked (UBPYflox), and the deleted (ΔUBPY) alleles. Filled boxes indicate exons (E2-E5). Arrowheads indicate loxP sites. Restriction enzyme sites and the location of the probe used for Southern blot analysis are depicted. *Nco*I fragments are in kilobases. N, *Nco*I. (B) Southern Blot of *Nco*I digested genomic DNA using a ^{32}P-labeled probe in sorted thymocytes (upper panel) and in sorted peripheral T cells (lower panel) from wildtype (WT) and UBPY $^{flox/flox}$/CD4 cre^{+} mice (KO). MLN, mesenterial lymph nodes. Data are representative of $n = 3$ pooled mice. (C) Graphic representation of UBPY-deletion rates in thymocyte subsets and peripheral T cell populations in UBPY $^{flox/flox}$/CD4 cre^{+} mice. For quantification of the UBPY deletion, the relative density of the 6kb band was measured using the ImageQuant software (Molecular Dynamics) and expressed as percentage of the density of all bands in each lane. (D) Immunoblot of UBPY deletion in total thymocytes and sorted CD4+CD8+ double positive thymocytes.

5.2 Spontaneous development of inflammatory bowel disease in UBPYΔ^T mice

UBPYΔ^T mice were born at the expected mendelian frequency and were kept under standard specific pathogen-free conditions. As early as six weeks of age, they developed signs of colitis, including diarrhea and rectal prolapse. The animals became rapidly wasted and moribund and all mice died within 20 weeks (Fig.5.2A). Gross examination of the organs of UBPYΔ^T mice, which already developed signs of disease, revealed a thickening of the bowel wall (Fig.5.2B). This was usually accompanied by splenomegaly, lymphadenopathy and sometimes, probably depending on progression of the disease, thymic loss. Histologically, the most prominent phenotypical changes were found in the colon. Hematoxylin/eosin staining of sections of the colon revealed a massive hyperplasia of the mucosa in UBPYΔ^T animals. Crypt abscesses could also be detected as well as a massive cellular infiltration (Fig.5.2C) in the lamina propria of UBPYΔ^T mice. In order to determine the nature of these infiltrating cells, colonic sections of wildtype and UBPYΔ^T mice were stained by immune histology with antibodies directed against CD3 as a T lymphocyte specific marker and FoxP3 as a marker for regulatory T cells. These stainings clearly showed that the infiltrating cells were essentially CD3 positive T cells (Fig.5.2D), with some interspersed regulatory T cells (Fig.5.2D, inset, arrow). No chronic inflammatory changes were detected in any other organ (data not shown). These mice were of mixed genetic backgrounds, which may have contributed to variations in disease progression in individual mice. There was no colitis in heterozygous or control (UBPY$^{wt/wt}$cd4cre^{+}, UBPY$^{wt/flox}$cd4cre^{+}, UBPY$^{flox/flox}$CD4cre^{-}) UBPYmice.

The colon pathology in the absence of chronic inflammatory changes in other organs in UBPYΔ^T mice is characteristic for inflammatory bowel disease (IBD), a chronic inflammation

of the mucosa. As a general rule, IBD is the result of an inappropriate response of the immune system towards the normal microflora of the gut. Several factors influence the development of the disease and similar clinical features appear in many mouse strains with diverse genetic defects (reviewed in [76]). A genetic predisposition of the mouse strain used determines whether a given genetic defect leads to the development of colitis or not. Second, the gut microflora is required for triggering or maintenance of the inflammation. Mice kept under germ-free conditions usually do not develop IBD. Genetic abnormalities in epithelial cells, for example, leading to the loss of their barrier function towards lumenal microorganisms can lead to colitis. Mucosal inflammation can also be due to genetic defects in cells of the adaptive immune system, if affecting the function of antigen-presenting cells, macrophages or natural killer cells. However in UBPYΔ^T animals, the defect must reside within the T cell population. In that case IBD results either of excessive effector function or defective regulatory T cell function. An excessive effector function is caused for example by an intrinsic overproduction of proinflammatory cytokines such as TNFα (i.e. TNF^{ARE} mice, [77]), or IFNγ (i.e. Stat4 transgenic mice, [78]). A defective regulatory function might be due to a failure to produce regulatory cytokines (i.e. IL-10 [79]) or to a defect in the development of regulatory T cells (i.e. IL-2 knockout mice, [80]). Immune histological stainings of colonic sections from UBPYΔ^T mice against FoxP3 revealed the presence of at least some regulatory T cells. Therefore the colitis in these mice is not due to the absence of regulatory T cells. In order to confirm that the pathological changes in UBPYΔ^T mice are indeed caused by a disturbance of immune homeostasis, we proceeded with the analysis of the peripheral T cells.

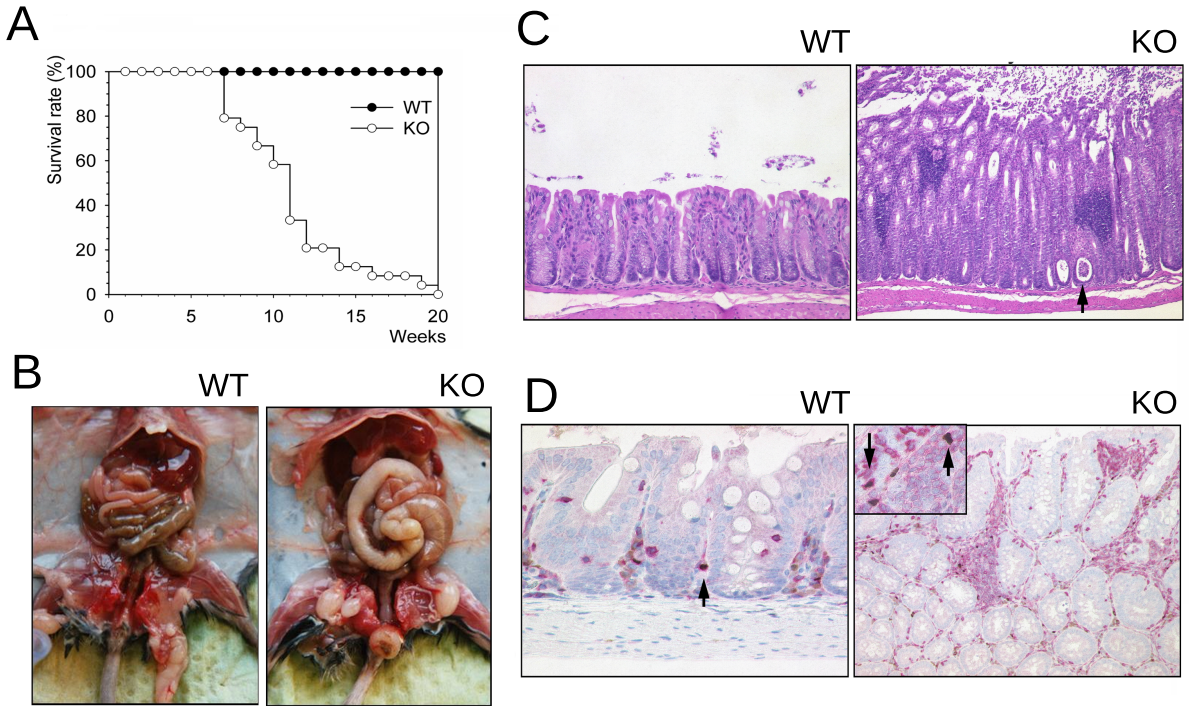

Figure 5.2: UBPYΔ^T mice develop an inflammatory bowel disease and die prematurely. (A) Survival curve of wildtype and UBPYΔ^T showing the lethality of the UBPYΔ^T phenotype. (B) Anatomy of WT and UBPYΔ^T animals showing the thickening of the colon and the rectal prolapse in UBPYΔ^T mice. (C) Histological analysis of colonic mucosa. The figure shows hematoxylin and eosin staining of colons from wildtype (WT, left) and UBPYΔ^T (KO, right) mice. Left, normal crypt architecture in wildtype (WT) animals. Right, in UBPYΔ^T (KO) mice, marked mucosal thickening and epithelial hyperplasia and elongated crypts. Some crypt abscesses (arrow). Cellular infiltrates. (D) Immune histological staining of colonic section from wildtype (WT) and UBPYΔ^T (KO) animals with antibodies directed against CD3 (red) and FoxP3 (brown). Visible are the infiltrates of CD3 positive cells in the lamina propria. The inset in the right box highlights the presence of FoxP3+ regulatory T cells in UBPYΔ^T animals (arrow).

5.3 Frequency and activation state of UBPYΔ^T peripheral T cells

To detect disturbances in immune homeostasis, first frequencies and total cell numbers of the peripheral T cells in young (4-6 weeks of age) wildtype (WT) and UBPYΔ^T (KO) mice were determined. At this age, UBPYΔ^T mice still had a healthy appearance, without the typical symptoms of colitis (rectal prolapse, diarrhoe and weight loss). Cells from lymph nodes and spleens were stained with fluorescent labeled antibodies against B220, a B lymphocyte specific marker, CD3, specific for T lymphocytes, CD4 and CD8 and the stained cells were analyzed by Flow Cytometry. The total numbers of the different lymphocytes subsets (B cells, T cells, CD4+ and CD8+ lymphocytes) in the spleen were calculated using the frequencies determined by Flow Cytometry. Fig.5.3A shows the results obtained by Flow Cytometry with the frequencies obtained. Fig.5.3B allows the comparison of total lymphocyte numbers in WT and KO spleens. While the frequency and numbers of B lymphocytes, characterized by the expression of B220, were unchanged, staining against CD3 revealed a significant reduction of the mature CD3+ T lymphocyte compartment. This reduction was detectable in both spleen and lymph nodes. Staining with anti-CD4 and anti-CD8 antibodies showed that both CD4+ and CD8+ T lymphocyte compartments were affected in spleen and lymph nodes. However the reduction was more severe in the CD4+ compartment, leading to an altered CD4:CD8 ratio of 0,9 in UBPYΔ^T mice compared to 1,5 in wildtype animals (Fig.5.3B).

Peripheral T cells had lower surface levels of TCR, as determined by staining with antibodies against TCRβ and quantification by Flow Cytometry (Fig.5.3C). In the spleen there even seemed to be a distinct CD4$^+$TCRβ^- population.

Next, the activation state of the peripheral T cells was analyzed. Splenocytes and lymph node cells were stained with antibodies against the positive activation markers CD69 and CD25 and

the negative activation marker CD45RB and analysed by Flow Cytometry. Fig.5.3C shows the overlays of the signals obtained with these markers in CD4+ cells from spleen and lymph nodes of wildtype and UBPYΔ^T mice. Surface expression of CD25 and CD69 was increased and surface expression of CD45RB was reduced in knockout animals, indicating a hyperactivated state of the peripheral T cells. Using the surface markers CD44 and CD62L it is possible to differentiate between naïve T cells (CD44^{low}CD62L^{high}), memory T cells (CD44^{high}CD62L^{high}) and effector T cells (CD44^{high}CD62L^{low}). The frequencies obtained were used to calculate the total numbers of these T cell subsets. Fig.5.3D shows that in CD4+ compartments of UBPYΔ^T lymph nodes, the frequency of naïve and memory T cells was drastically reduced, with the large majority of the T lymphocytes bearing an effector phenotype.

The analysis of the peripheral T lymphocyte populations shows that UBPY knockout in T cells leads to a severe lymphopenia in UBPYΔ^T animals. Clearly, immune homeostasis is disturbed, with the few remaining T lymphocytes being aberrantly high activated and mostly displaying an effector phenotype, while naïve T cells are almost absent. Hyperactivation is already detectable at 4 weeks of age, and therefore precedes onset of the colitis. The T cells in UBPYΔ^T mice have reduced surface levels of T cell receptor. This might reflect the hyperactivated state of the T cells, resulting in enhanced ligand induced downmodulation or alternatively might be caused by a maturation defect during thymocyte development. Disturbed T cell development could also be causative for the overall reduction of the T lymphocyte populations. Therefore the next step consisted in the detailed analysis of thymocyte development in UBPYΔ^T mice.

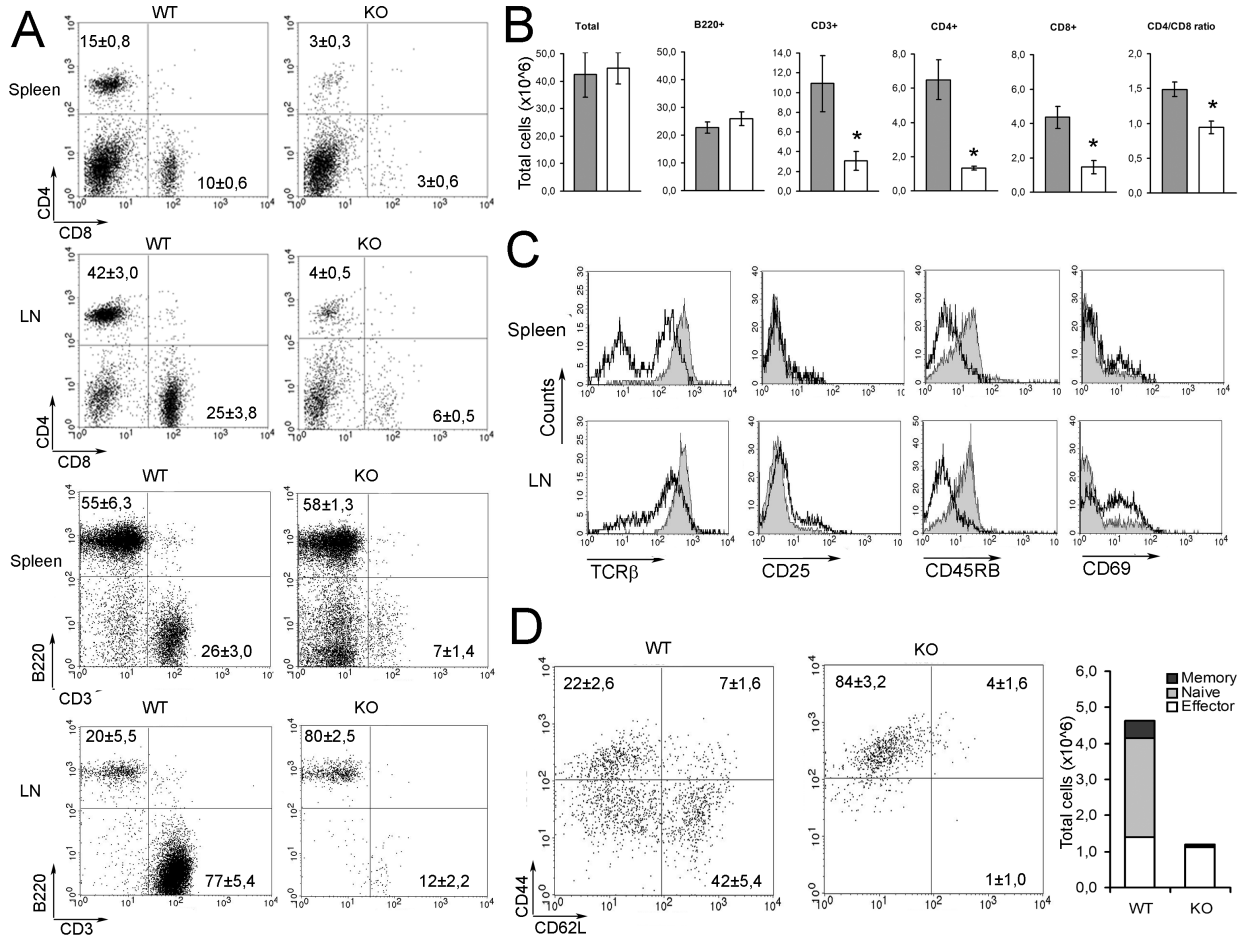

Figure 5.3: Lymphopenia and hyperactivation of peripheral T cells in UBPYΔ^T mice. (A) Flow cytometry of lymphocyte subsets in spleen and lymph nodes (LN) from 6-week-old wildtype (WT) and UBPYΔ^T (KO) mice after staining with antibodies against CD3, B220, CD4 and CD8 as indicated. . Numbers in quadrants indicate the frequency of subpopulations (mean$\pm$sem of $n \geq 3$). (B) Total numbers of lymphocyte subsets (horizontal axes) in spleens from 6-week-old WT mice (gray bars) and UBPYΔ^T mice (open bars), mean$\pm$sem of $n \geq 3$, asterisks (*) indicate statistically significant differences ($p \leq 0,02$). (C) Flow cytometry of activation markers CD25, CD69 and CD45RB and TCRβ chain in CD4+ T cells from spleen and lymph nodes(LN) of wildtype (filled histograms) and UBPYΔ^T (open histograms) mice. Results are representative of at least three independent experiments. (D) Flow Cytometry of functional subpopulations in splenic CD4+ T cells of wildtype (WT) and UBPYΔ^T (KO) animals. Numbers in quadrants indicate frequencies of naïve (CD44^{low}CD62L^{high}), effector (CD44^{high}, CD62L^{low}) and memory (CD44^{high}CD62L^{high}) T cell subsets (mean $\pm$ s.e.m.; $n \geq 4$, 4-8week old mice). Total numbers of the functional subpopulations in splenic CD4+ T cells were calculated using the frequencies obtained by Flow Cytometry and represented in the stacked columns diagram on the right. Dark gray, memory T cells; light gray, naive T cells; white, effector T cells.

5.4 Thymocyte development in UBPYΔ^T mice

In order to analyse the development of the thymocytes, the thymi of 4-6 weeks old UBPYΔ^T animals and wildtype controls were removed and single-cell suspensions prepared. The different thymocyte subsets were stained with antibodies coupled to fluorescence markers and analysed by Flow Cytometry: CD4 and CD8 antibodies were used for the four main thymocyte subsets. The DN stages were analysed using antibodies against the surface markers CD4, CD8, CD44 and CD25. The TCR$\gamma\delta$ thymocytes were determined as the CD3+TCR$\gamma\delta$+ subset by staining with CD3 and TCR$\gamma\delta$ antibodies. The regulatory T cell subset was defined as the CD8-CD4+CD25+ subset by staining with antibodies against these three surface markers. Total thymocyte numbers were counted and total numbers of the thymocyte subsets calculated using the frequencies obtained by Flow Cytometry (Fig.5.4C). The analysis of the CD4 and CD8 expression showed significantly reduced frequencies of CD4+ and CD8+ single positive (SP) compartments, by similar frequencies of the double negative compartment and increased frequency of the double positive compartment (Fig.5.4A, upper panel). The CD25 and CD44 expression in the DN compartment revealed that the DN stages are not affected in UBPYΔ^T animals (Fig.5.4A, lower panel). Also the frequency of the TCR$\gamma\delta$ subset of thymocytes was not affected by the UBPY knockout (Fig.5.4B, upper panel). Frequency and numbers of CD8-CD4+CD25+ cells within the hole thymocyte compartment were reduced (Fig.5.4C). This was not surprising, given the overall reduction in CD8-CD4+ cells in UBPYΔ thymocytes. The percentages of CD4+CD25+ cells within the CD8- compartment however were similar in wildtype and UBPYΔ mice (Fig.5.4B, lower panel). Total thymocyte numbers in young, preclinical UBPYΔ mice were not altered in comparison to wildtype animals. This confirms the presumption that thymic loss observed in several UBPYΔ mice in later stages of the colitis is a disease associated symptom. Numbers of thymocyte subsets therefore reflected the differences in frequencies: there was a significant

reduction of CD4 single positive thymocytes, including the regulatory T cells, and CD8 single positive cells, while total numbers of double negative, double positive and TCR$\gamma\delta$ thymocytes were unchanged in UBPYΔ mice (Fig.5.4C). The reduction in numbers in UBPYΔ SP thymocytes was more drastic in the CD4SP compartment than in the CD8SP compartment, resulting in a ratio of CD4SP to CD8SP of 0,9 compared to 1,8 in wildtype animals. These results indicate a maturation defect in UBPYΔ thymocytes, leading to a block in thymocyte development at the double positive stage.

To further investigate that thymic defect, the expression of the developmental stage specific surface markers CD5, CD3ϵ, CD69 and CD24(heat shock antigen, HSA) was analysed by Flow Cytometry (Fig.5.5A). CD5 is expressed at very low levels on early DN thymocytes, however signals transduced by the pre-TCR upregulate CD5 and the levels of CD5 expression reflect the extent or intensity of pre TCR signaling [81]. At the DP stage most thymocytes express intermediate levels of CD5 and low TCR signals are sufficient to maintain this expression. Only those DP thymocytes that express TCRs that can interact with MHC-ligand with sufficiently high affinity to promote either positive or negative selection upregulate CD5 surface expression to high levels. DP thymocytes express low levels of TCR and TCR levels are upregulated after receipt of a selecting TCR signal, bearing SP thymocytes with ten-fold increased surface levels. CD69 is used as a marker to identify the thymocytes that are auditioning in positive selection. CD69 upregulation is initiated after TCR and CD5 upregulation and is crucially dependent upon TCR$-$MHC$-$peptide interactions[82]. HSA is used as a marker for the late stage of SP thymocyte maturation [83] and downregulation of HSA correlates with increasing maturation. The SP thymocytes with no expression of HSA at their surface are the most mature thymocytes and ready for emigration to the periphery. At the DN developmental stage, UBPYΔ^T thymocytes expressed normal quantities of CD3ϵ, CD69 and CD24. CD5 expression however was lower,

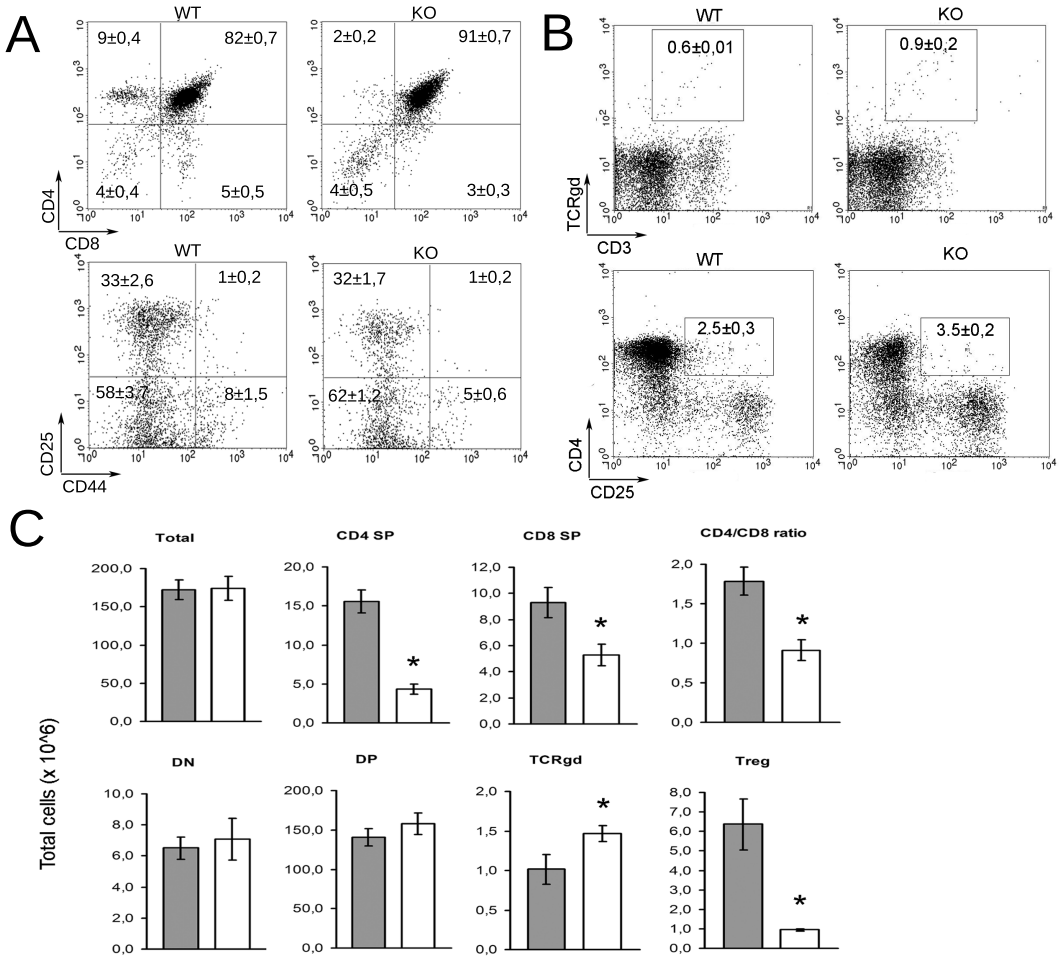

Figure 5.4: Defective thymocyte development in UBPYΔ^T mice. (A-B) Thymocyte subsets from 6-week-old wildtype (WT) and UBPYΔ^T mice (KO) were analyzed by Flow Cytometry. Numbers in quadrants and in boxed areas indicate the frequency of subpopulations (mean$\pm$sem). (A) Upper panel, frequencies of the four main thymocyte subsets classified by expression of CD4 and CD8, $n = 9$. Lower panel, frequencies of double negative stages classified by expression of CD44 and CD25 in the CD4$^-$CD8$^-$ gate ($n = 4$). (B) Upper panel, frequencies of the TCR$\gamma\delta$ thymocytes, ($n = 3$). Lower panel, frequencies of regulatory T cells, determined as CD4+CD25+ cells within the CD8- gate, ($n = 3$). (C)Total numbers of thymocyte subsets (horizontal axes) in 6-week-old WT mice (gray bars) and UBPYΔ mice (open bars)are represented as mean$\pm$sem, asterisks (*) indicate statistically significant differences ($p \leq 0,02$)

suggesting a defective pre-TCR signaling. This is not in contradiction to the normal DN-DP transition in UBPYΔ^T, since CD5 expression is not required for thymocyte maturation [84]. No significant differences in the expression of any of the the four markers could be detected between DP thymocytes of wildtype and UBPYΔ^T mice, probably due to the fact that positively selected thymocytes constitute only a minor fraction of the DP subset. By contrast, in the CD8SP compartment, CD5, CD3ϵ and CD69 expression were drastically reduced, while a mild reduction was observed in CD4SP thymocytes. The most mature CD4SP and CD8SP thymocyte subsets, characterised by low expression of HSA are almost lacking in UBPYΔ^T thymocytes.
Several studies showed that UBPY has an essential role in cell proliferation with lack of UBPY inducing a growth arrest in several cell lines [8, 9]. The defective development of thymocytes in UBPYΔ^T animals was therefore likely to be caused by a defect in cell cycle progression. In order to test this, mice were injected intraperitoneally with BrdU, a thymidine analogue, that is incorporated into the newly synthesized DNA of replicating cells during the S phase of the cell cycle. Two hours after injection, the mice were sacrificed and the BrdU incorporation in the thymocyte subsets was assessed with a BrdU-specific antibody by Flow Cytometry (Fig.5.5B). The percentages of BrdU incorporating, thus replicating cells in the thymocyte subsets of UBPYΔ^T animals were not reduced compared to control animals. Within the CD8 single positive compartment this percentage was even highly increased, probably reflecting the highly immature phenotype of this subset in UBPYΔ^T animals. These results clearly show that, in thymocytes, lack of UBPY does not induce cell cycle arrest and that the defect in thymocyte development is not caused by impaired cell proliferation.

UBPYΔ^T animals are clearly impaired in thymocyte development, leading to a severe reduction of frequencies and absolute cell numbers in both single positive departments. The lower CD4:CD8 ratio indicates that the CD8SP compartment is less severely affected, in terms of

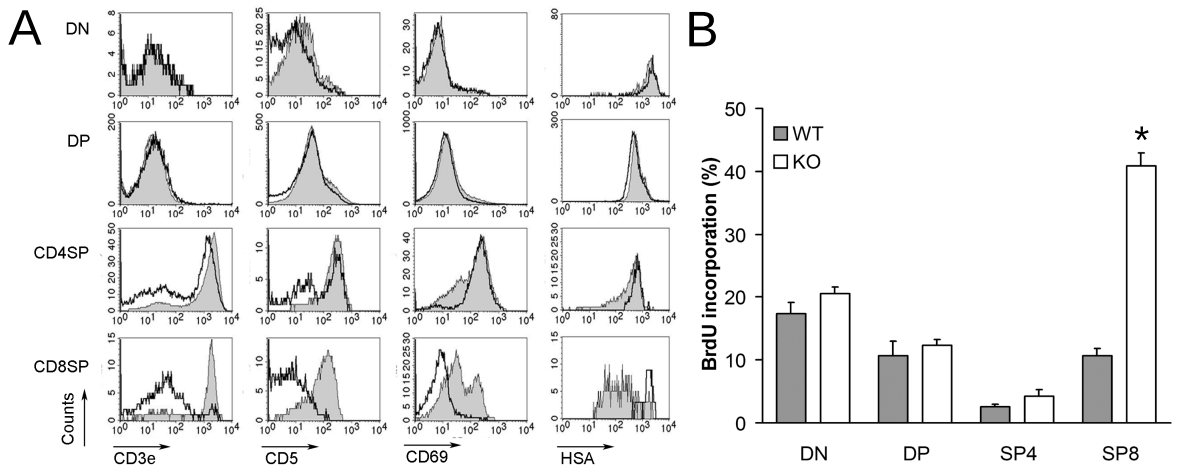

Figure 5.5: Impaired thymocyte maturation in UBPYΔ^T mice. (A) Flow Cytometry of differentiation markers CD5, CD69, CD24 and CD3ϵ in thymocyte subsets of WT(filled histograms) and UBPYΔ^T animals (open histograms). The histogram overlays are representative of at least three independent experiments. (B) *In vivo* BrdU incorporation in thymocyte subsets (horizontal axis) of 4-week-old mice wildtype mice (WT, gray bars) and UBPYΔ^T mice (KO, open bars), presented as mean $\pm$ s.e.m. ($n = 6$ mice per group). The asterisk (*) indicates statistically significant difference ($p \leq 0,0005$)

frequencies and numbers. However the analysis of the maturation markers shows that this compartment in UBPYΔ^T mice mainly consists of immature CD8SP cells. Analysis of different developmental markers revealed that additionally to the reduction in numbers of SP thymocytes, UBPYΔ^T mice have a drastic thymocyte maturation defect yielding SP thymocytes with low surface TCR expression and high expression of HSA. The lower expression of CD5 and CD69 in UBPYΔ^T SP thymocytes , markers whose expression is proportional to the signals received through the TCR, suggests a defective signaling through the TCR.

The selection processes, lineage commitment and maturation steps during thymocyte development, which are affected in UBPYΔ^T mice, all depend on tightly balanced responses to TCR stimulation. The next step therefore consisted in the analysis of the responsiveness of UBPYΔ^T thymocytes to stimulation through the TCR.

5.5 UBPYΔ^T thymocytes exhibit a defective responsiveness to TCR stimulation

Developing thymocytes are destined to die by apoptosis, unless interaction of the TCR with MHC-self-antigen complexes induces a rescue signal leading to proliferation of the cell. To determine the responsiveness of UBPYΔ^T thymocytes to TCR stimulation three read-outs were therefore used: the proliferation rate, the rate of apoptosis induction and the amount of the growth factor interleukin-2 produced.

For assessment of the proliferation rate *in vitro*, thymocytes of 6 week old wildtype and UBPYΔ^T mice were seeded in triplicates on 96-wells plates coated with increasing concentrations of plate-bound anti-CD3 antibody and with or without addition of recombinant mouse Interleukin-2 for four days at 37°C. Twelve hours before acquisition the cells were loaded with ^{3}H-labeled thymidine. At the end of the incubation period, the cells were harvested on filter plates and incorporation of the radioactive thymidine measured in a scintillation counter. Since only proliferating cells are capable of incorporating the ^{3}H-thymidine, the scintillations count is directly proportional to the proliferation rate in a sample.

A depicted in Fig.5.6A, after this *in vitro* incubation period and independently of the concentration of plate-bound CD3 antibody used, no proliferation of UBPYΔ^T thymocytes could be detected in the absence of Interleukin-2, while the proliferation rate in wildtype thymocytes raised with increasing concentrations of anti-CD3. However the proliferation rate in UBPYΔ^T thymocytes was restored almost to wildtype level by addition of recombinant Interleukin-2 to the medium. IL-2 is a crucial regulator of T cell proliferation, survival and programmed cell death (apoptosis) (reviewed in [85]). However, at low concentrations, IL- 2 prevents apoptotic death of thymocytes induced by CD3-stimulation *in vitro* [86]. The reduced proliferation rate *in vitro* of UBPYΔ^T thymocytes therefore might result from an increased susceptibility to apoptotic death.

Viability of wildtype and UBPYΔ^T thymocytes with or without TCR stimulation was therefore compared. In a survival assay, thymocytes were incubated without stimulating agents for 0h, 24h and 48h. At each time point, cells were stained with the apoptosis marker Annexin V and a vital dye, Propidium iodide (PI). Vital cells were identified as AnnexinV^-PI^- cells and their frequencies determined (Fig.5.6C). This survival assay shows that there are no differences in the viability of wildtype and UBPYΔ^T thymocytes without TCR stimulation. Next, apoptosis induction was tested by incubating thymocytes with plate-bound CD3 antibodies and soluble CD28 antibodies for 24h. After this incubation, the thymocytes were stained with fluorescent coupled Annexin V and the vital dye Propidium iodide (PI) and analysed by Flow Cytometry. Annexin V has a high affinity towards phosphatidylserine, a phospholipid of the plasma membrane. The translocation of PS from the inner to the outer leaflet of the plasma membrane, making it accessible to Annexin V, is one of the very first indications of apoptosis. Propidium iodide binds to nucleic acids, but can only penetrate the plasma membrane when membrane integrity is breached, as occurs in the later stages of apoptosis or in necrosis. Cells in early apoptosis are therefore stained by Annexin V, but not by Propidium iodide, in contrast to cells in late apoptosis or dead cells, which are stained by both. The results of this assay showed no differences in the susceptibility to apoptosis after *in vitro* stimulation between wildtype and UBPYΔ^T thymocytes (Fig.5.6D).

To test the ability of UBPYΔ^T thymocytes to produce interleukin-2, single-cell thymocyte suspensions were prepared and seeded in 96-well plates with plate-bound CD3 antibodies for 72hours. Concentrations of Interleukin-2 in the cell supernatants were then tested by ELISA. This assay revealed that UBPYΔ^T thymocytes do not produce detectable levels of Interleukin-2 in response to stimulation with anti-CD3 antibodies(Fig.5.6B).

These results show that UBPYΔ^T thymocytes have a disturbed responsiveness to TCR stimulation*in vitro*, as detected by the absence of proliferation and of interleukin-2 production. This seems not to be caused by a decreased viability or an increased susceptibility to apoptosis of the

UBPYΔ^T thymocytes *in vitro*. Consequently, in the next steps, the regulation of TCR surface levels and the TCR signal transduction pathways were evaluated.

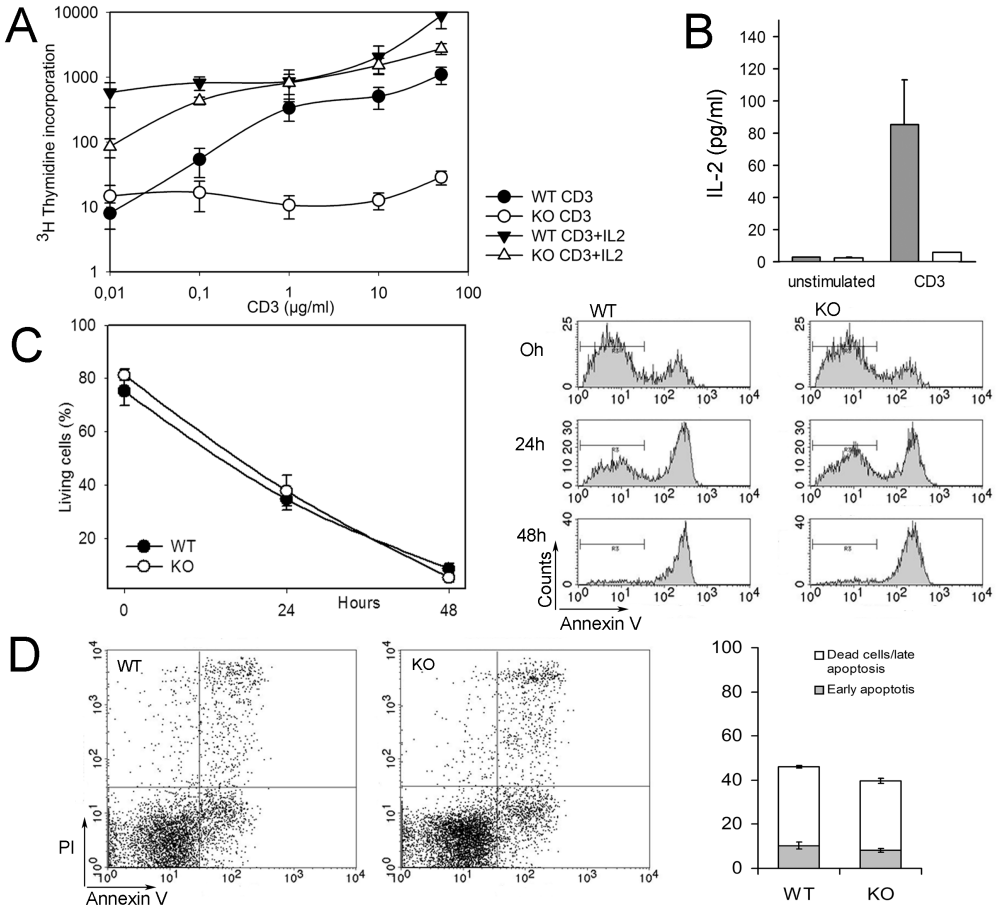

Figure 5.6: Impaired responsiveness of UBPYΔ^T thymocytes to TCR stimulation. (A)Proliferation assay. *In vitro* ^{3}H Thymidine incorporation in thymocytes of 6-week-old wildtype (WT, black circles) and UBPYΔ^T (KO, open circles) after stimulation with increasing concentrations of plate-bound CD3 antibody (in μg/ml) and with or without addition of recombinant mouse Interleukin-2 (100u/ml) for 96h. Representative of two independent experiments with $n = 3$ mice each. (B) Il-2 production in thymocytes from 6-week-old WT (gray bars) and UBPYΔ^T (open bars) mice ($n = 3$) with or without stimulation with plate-bound anti-CD3 antibody for 72h, determined by ELISA. (C)Survival assay. Thymocytes from wildtype (WT) and UBPYΔ^T (KO) mice were incubated for the indicated times in medium without stimulating agents, stained with fluorescent coupled apoptosis marker Annexin V and the vital dye propidium iodide (PI) and analysed by Flow Cytometry. Left, frequencies of living cells (AnnexinV$^-$PI$^-$) in WT(black circles) and KO(open circles) thymocytes over time (mean$\pm$sem of $n = 4$ mice). Right, Annexin V staining in the PI$^-$ gate of WT and KO thymocytes after t=0h, 24h and 48h incubation. (D)Stimulation induced apoptosis. Thymocytes from wildtype (WT) and UBPYΔ^T (KO) mice were incubated for 24h with plate-bound anti-CD3 antibody and soluble anti-CD28 antibody, stained with fluorescent coupled apoptosis marker Annexin V and the vital dye propidium iodide (PI) and analysed by Flow Cytometry (Left). Cells in early apoptosis were determined by Annexin V$^+$PI$^-$ staining, cells in late apoptosis and dead cells were detected by Annexin V$^+$PI$^+$ staining. Right, frequencies of early and late apoptotic cells in wildtype (WT) and UBPYΔ^T (KO) thymocytes (mean$\pm$sem, $n = 5$).

5.6 Normal intracellular trafficking of TCR in UBPYΔ^T thymocytes

Analysis of the thymocyte development in UBPYΔ^T mice indicated that UBPYΔ^T thymocytes fail to upregulate the T cell receptor (TCR) surface levels during their maturation to single positive (SP) thymocytes. The analysis of three TCR components, the TCRβ, CD3ϵ and CD3ζ chains, in the different thymocyte subsets by Flow Cytometry showed that all three are expressed at lower levels in UBPYΔ^T SP thymocytes compared to wildtype (Fig. 5.7A), with the exception of the CD3ζ chain, whose expression in CD4SP, but not in CD8SP, thymocytes equaled wildtype levels. Several publications showed that UBPY plays an important role in endosomal trafficking of receptor tyrosine kinases such as the EGFR [9, 11, 10], with a drastic reduction of EGFR levels in UBPY depleted cells [9]. Similar to receptor tyrosine kinases, TCR are constitutively internalized, but rapidly recycled back to the cell surface in order to maintain steady levels of surface TCR [64]. Upon ligand stimulation surface TCR levels are downmodulated, probably by increased targeting of the TCR for degradation in lysosomes instead of recycling [65]. Both EGFR and TCR modulation are mediated by ubiquitination through the activity of the E3 ligase cbl [69, 87]. Therefore low TCR surface levels in UBPYΔ^T SP thymocytes might be caused by a defective endosomal trafficking of the TCR.

In order to determine the TCR downmodulation rate after ligand stimulation, thymi from 6-week old wildtype and UBPYΔ^T mice were removed and single-cell suspensions prepared. After lysis of the erythrocytes, total thymocytes were stained with a biotinylated hamster anti-TCRβ antibody on ice. At $t = 0$ TCR were crosslinked by addition of an anti-hamster antibody and the cells were incubated at 37°C for different times. At t the reaction was stopped by addition of ice-cold PBS. The TCR remaining at the surface were stained with phycoerythrin(PE)- labeled streptavidin and PE-fluorescence measured by Flow Cytometry. Additional staining with fluorescent

labeled CD4 and CD8 antibodies allowed the gating on thymocyte subsets. For quantification of TCR downmodulation, the median fluorescence intensity (MFI) associated with TCR-antibody complexes at t was expressed as percentage of the MFI at $t = 0$ and plotted in function of time (Fig.5.7B). In both CD4SP and DP thymocyte subsets the MFI from the surface TCR decreased over time, indicating a successful downmodulation after ligand stimulation. However there was no difference between wildtype and UBPYΔ^T thymocytes. This result clearly shows that UBPY is not involved in the regulation of ligand induced TCR downmodulation.

For analysis of the ligand-independent dynamics, thymocytes from wildtype and UBPYΔ^T mice were incubated for various times in medium alone (unstimulated controls), in medium supplemented with Brefeldin A (10μg/μl) or in medium supplemented with cycloheximide (50μg/μl)at 37°C to allow trafficking of the TCR. At each time point the reaction was stopped by addition of ice-cold PBS (phosphate buffered saline) and the samples stored on ice until all samples were collected. Then the thymocytes were stained with fluorescent coupled antibodies against TCRβ, CD4 and CD8 at 4°C and the fluorescence associated with TCRβ in the DP and CD4SP gates quantified by Flow Cytometry. The percentages of TCR downmodulation under the different conditions in the DP or CD4SP subset (Fig.5.7D) were determined from the median fluorescence values using the unstimulated controls as reference, or the median fluorescence value at $t = 0$ for the untreated samples themselves. Cycloheximide interferes with translation elongation and thereby blocks protein synthesis. Brefeldin A (BFA) severely alters the cellular organelle organization, leading to an extensive tubulation of endosomes, the trans-Golgi network (TGN) and the lysosomes. During BFA treatment, the Golgi mixes with the endoplasmatic reticulum leading to a blockage of the transport of newly synthesized proteins from the endoplasmatic reticulum to the Golgi complex [88, 89]. Additionally BFA induces fusion of the trans-Golgi network with early endosomes, which, although initially reported to leave cycling between plasma membrane and endosomes of transferrin unaffected [88], has meanwhile been shown to impair the endocytic

transport of the TCR [64, 90]. Incubation in medium only revealed that the TCR surface levels in CD4SP remained stable over the observed period of six hours, with no significant difference between wildtype and UBPYΔ^T mice. In contrast, in DP thymocytes the surface levels constantly increased up to 160% of SF_0 after six hours, with no difference between wildtype and UBPYΔ^T animals, probably reflecting the ongoing differentiation with TCR upregulation towards SP thymocytes of the DP subset. This result shows that surface TCR levels in UBPYΔ^T SP thymocytes are not *per se* instable. Treatment with cycloheximide had no effect on TCR expression in wildtype or UBPYΔ^T SP thymocytes, but lead to a drastic reduction of surface levels compared to untreated cells in DP thymocytes. Therefore, in contrast to surface expression in DP thymocytes, surface expression of the TCR in SP thymocytes is independent of newly synthesized complexes. In DP thymocytes, treatment with BFA had the same effect on TCR expression as treatment with cycloheximide, reflecting the importance of protein synthesis in this thymocyte subset, and probably masking the minor influence of endosomal trafficking. In SP thymocytes, the effect of BFA on TCR expression was different from that of cycloheximide and resulted in a partial reduction of TCR membrane levels of about 20% within the first hour, which was maintained for a couple of hours. However, after six hours, surface levels were restored again, probably due to a compensatory mechanism or incomplete action of Brefeldin A.

Neither treatment with Brefeldin A, nor treatment with cycloheximide revealed any differences in TCR surface modulation between wildtype and UBPYΔ^T thymocytes. From this it can be concluded that endosomal trafficking and synthesis rates of the TCR are not defective in UBPYΔ^T thymocytes. This was also supported by the observation that, in contrast to the aforementioned studies showing alterations in endosomal sorting in UBPY-depleted cells [9, 11, 10], the levels of Hrs and STAM were unaltered in UBPYΔ^T thymocytes (Fig5.7C). As altered responsiveness of UBPYΔ^T thymocytes might alternatively caused by defects in TCR signal transduction, the signal transduction pathways after TCR stimulation were analysed in the next chapter.

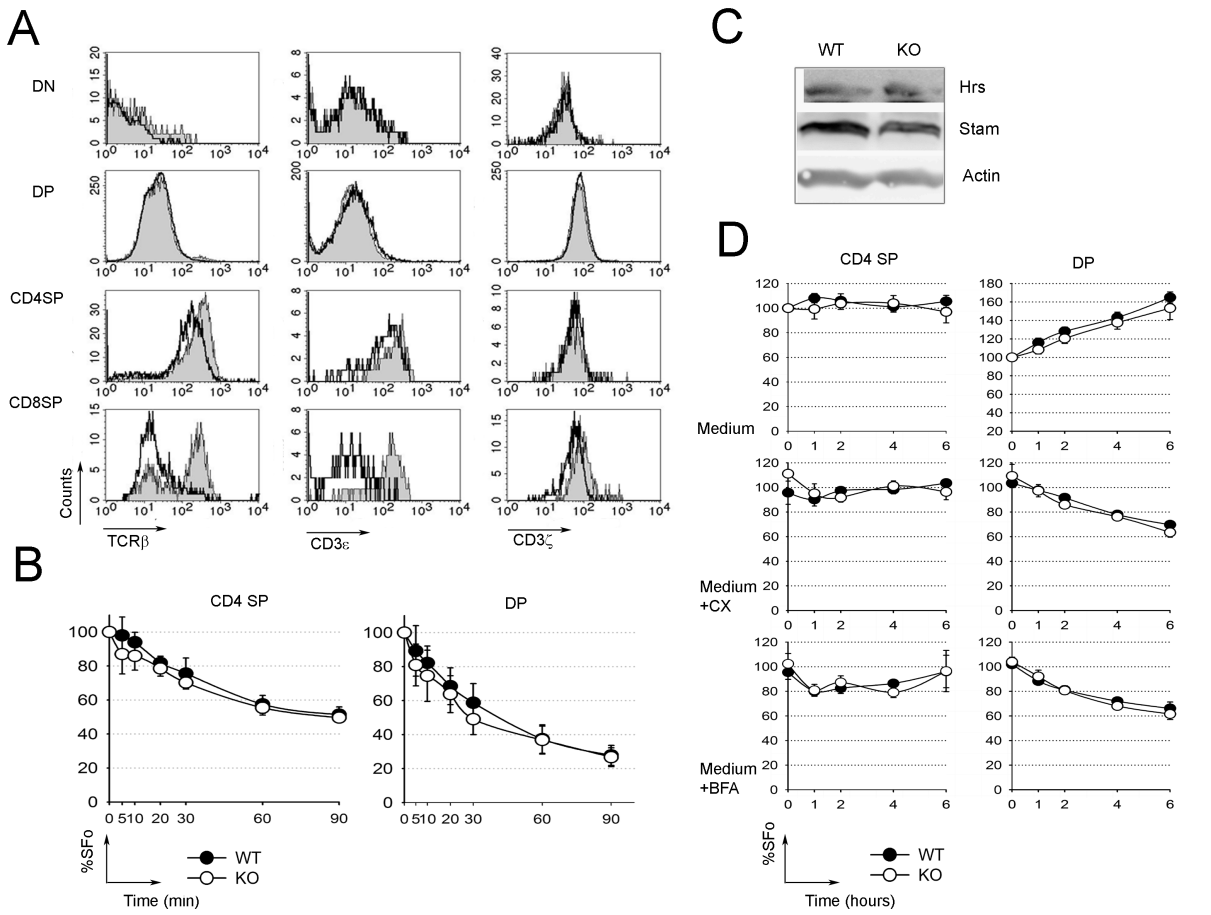

Figure 5.7: Regulation of TCR surface levels in UBPYΔ mice. (A) TCR surface expression. Flow cytometry of TCRβ, CD3ϵ and CD3ζ chains in thymocyte subsets of wildtype (WT, filled histograms) and UBPYΔ^T mice (KO, open histograms). DN, double negative, DP, double positive, SP single positive. (B) Ligand induced TCR downmodulation in wildtype (WT, filled circles) and UBPYΔ^T (KO, open circles) thymocytes. Thymocytes were stained on ice with biotinylated hamster anti-TCRβ, the TCR crosslinked with anti-hamster antibody and incubated at 37°C for the indicated times. At t remaining surface TCR were labeled with streptavidin-PE and measured by FACS in CD4SP(left) and DP(right) gates. The percentage of surface expression was determined from the mean fluorescence values of treated cells, using the untreated controls as reference. (mean $\pm$ s.e.m.; $n = 5$). (C) Western Blot of Hrs and STAM in total thymocytes from wildtype (WT) and UBPYΔ^T animals. (D) Ligand independent modulation of TCR surface levels in wildtype (WT, filled circles) and UBPYΔ^T (KO, open circles) thymocytes. Thymocytes were incubated for the indicated times in medium alone, in medium with 50μg/μl cycloheximide (CX) or in medium with 10μg/μl Brefeldin A (BFA). At t cells were stained with a fluorescent-coupled anti-TCRβ, anti-CD4 and -CD8 antibodies and TCR surface levels of gated CD4SP and DP thymocytes acquired by FACS. The percentage of surface expression was determined from the mean fluorescence values of treated cells, using the untreated controls as reference (mean $\pm$ s.e.m.; $n \geq 4$).

5.7 TCR signal transduction in UBPYΔ^T mice

The defective thymocyte development in UBPYΔ^T mice and the impaired responsiveness of UBPYΔ^T thymocytes suggested that UBPY might regulate TCR signaling.

To examine that possibility tyrosine phosphorylation induced by stimulation with CD3 and CD28 antibodies in wildtype and UBPYΔ^T thymocytes was analysed. For that, thymi from 6-week old mice were removed and single-cell suspensions prepared. The cells were resuspended in starving medium (RPMI 1640 medium with penicillin and streptomycin (P/S)) and incubated for 15 minutes at 37°C. After the starving incubation, cells were pelleted, resuspended in pre-warmed stimulation medium (RPMI with P/S, 10μg/ml CD3 antibody, 2μg/ml CD28 antibody and 10μg/ml anti-hamster IgG) and incubated at 37°C with moderate shaking (200rpm). At each time point a sample of the cell suspension was taken, immediately transferred into boiling SDS buffer and incubated at 95°C for 15 minutes with vigorous shaking (1000rpm). The resulting SDS protein samples were separated by SDS Page and analysed by Western Blot with specific antibodies. First, overall tyrosine phosphorylation was tested using a Phospho-tyrosine antibody (4G10) provided by Prof. Burkhardt Schraven from the University of Magdeburg (Fig.5.8A). Overall stimulation induced tyrosine phosphorylation was weaker in UBPYΔ^T thymocytes, particularly visible for the bands at 70kDa and $\approx$ 110kDa. In contrast to that, a band at $\approx$45kDa was stronger after 2 and 5 minutes of stimulation in UBPYΔ^T thymocytes compared to the wildtype(arrow). The tyrosine kinase ERK has two isoforms of 42 and 44 kDA. Therefore the phosphorylation of ERK1/2 after TCR stimulation was assessed in WT and UBPYΔ^T thymocytes by Western Blot using an antibody directed against ERK1/2 phosphorylated at Thr202 and Tyr204 of ERK1 (Thr185 and Tyr187 of ERK2). As shown in Fig.5.8B, ERK1/2 was indeed stronger phosphorylated in UBPYΔ^T thymocytes compared to wildtype after 2 minutes of TCR stimulation. Similarly LAT phosphorylation after 10 minutes of TCR stimulation was stronger

in UBPYΔ^T thymocytes compared to wildtype, while phosphorylation of Zap70 seemed unaffected. This enhanced signal, however, was only transient, as shown in Fig.5.8C. After 30minutes of TCR stimulation, ERK1/2 phosphorylation of UBPYΔ^T thymocytes was markedly lower compared to wildtype thymocytes. LAT phosphorylation in UBPYΔ^T thymocytes dropped to wildtype levels after 60 minutes of TCR stimulation. Analysis of the immediate early gene c-Fos showed that the aberrant ERK signal in UBPYΔ^T thymocytes was not able to induce wildtype expression levels of this factor.

It was suggested that deubiquitinating enzymes were functionally linked to E3 ligases due to the coevolution of the two groups of enzymes [23], with the deubiquitinating enzymes being responsible for stabilization of E3 ligases by counteracting their autoubiquitination. In an attempt to find a substrate of UBPY the constitutive expression levels of several E3 ligases, of components of the early TCR signaling complex and the overall pattern of ubiquitination RIPA protein extracts of wildtype and UBPYΔ^T thymocytes were tested (Fig.5.8D). In contrast to the published UBPY knockout models in different cell lines [9, 11], UBPY knockout in thymocytes did not lead to an accumulation of ubiquitinated substrates. However, for none of the E3 ligases tested, a destabilization in UBPYΔ^T thymocytes could be observed. Also, all the components of the early TCR signaling complex tested displayed unaltered levels in UBPYΔ^T thymocytes, implicating that the aberrant TCR signaling in UBPYΔ^T thymocytes is probably not caused by an altered composition of the early TCR signaling complex.

These results provide evidence for a specific role of UBPY in TCR signal transduction, with lack of UBPY leading to stronger, but more transient ERK phosphorylation. These altered kinetics of the TCR signal are probably not caused by a destabilization of the TCR signaling complex, suggesting a degradation-independent effect of deubiquitination by UBPY on TCR signaling.

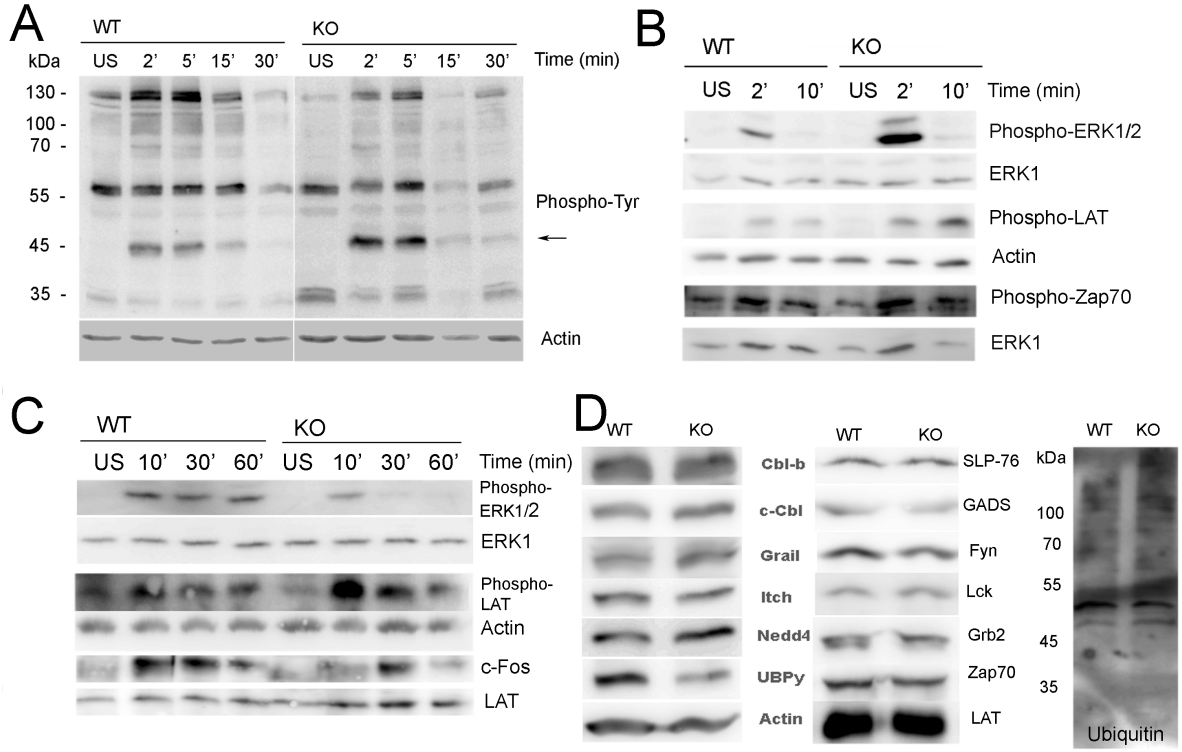

Figure 5.8: Aberrant TCR signal transduction in UBPYΔ^T mice. (A-C) Total thymocytes from 6-week old wildtype (WT) and UBPYΔ^T mice were left untreated (US) or were stimulated with anti-CD3 (10μg/ml), anti-CD28 (2μg/ml)and cross-linked with anti-hamster IgG (10μg/ml). At the times indicated (above lanes) total protein extract were produced by transferring the cells in boiling SDS sample buffer and the samples subjected to immunoblot analysis. (A) Total protein phosphorylation was analysed by immunoblot with a phospho-tyrosine specific antibody (Phospho-Tyr). The arrow indicates a band with stronger, but more transient phosphorylation. (B) Phosphorylation of ERK1/2, LAT and Zap70 at early time points. (C) Phosphorylation of ERK1/2 and LAT and expression of c-Fos at later time points (detected by high exposure of the immunoblots). (D)Immunoblot analysis of E3 ligases, of components of the early TCR signaling complex and of the ubiquitination pattern in RIPA total protein extracts of untreated wildtype (WT) and UBPYΔ^T (KO) thymocytes. 100μg protein extract/lane, antibodies are indicated on the left side of the blots. Actin was used as loading control and deletion was confirmed with UBPY specific antibody.
Data (A-D) are representative of at least three experiments.

Chapter 6

Discussion

6.1 Successful generation of a T cell specific knockout model for the *in vivo* study of UBPY function

The function of the isopeptidase UBPY has been studied in several cell culture models using different knock-down strategies, from antisense RNA[8] to siRNA[11, 10], overexpression of dominant negative mutants[50] or cre-induced deletion of the loxP-flanked gene[9], all in immortalized cell lines. These studies agreed on a role of UBPY in cell proliferation [8, 9], with UBPY deletion leading to a growth arrest. Also, the accumulation of ubiquitinated substrates at the endosomes associated with aberrant enlargement was congruently observed by several independent work groups[11, 10, 9, 50], establishing UBPY as an important factor in trafficking of ubiquitinated substrates to endosomes and lysosomes. Endosomal trafficking plays a central role in T cell development and function. Since UBPY was also reported to interact with a major player in TCR signaling, the adaptor molecule GADS [12], and with a central regulator of T cell anergy, the E3 ligase GRAIL [13], this lead us to investigate the role of UBPY in T cells. How-

ever, the conventional knockout turned out to be embryonically lethal and cre-mediated induction of overall UBPY deletion in adult mice lead to their rapid death due to a severe liver failure, thus limiting the use of primary material from these mouse models [9]. This work attempted to circumvent these difficulties by establishing a mouse line bearing the UBPY knockout only in T cells. The previously described [9] UBPY$^{flox/flox}$ mouse line was crossed to a transgenic mouse strain expressing the cre recombinase under the control of the CD4 promoter. The resulting UBPY$^{flox/flox}$CD4cre^{+} (UBPYΔ^{T}) mice effectively deleted UBPY in thymocytes starting from double negative stage 4 with the highest deletion rate of around 80% in double positive thymocytes (Fig.5.4B). The mice also yielded mature UBPY deleted T cells, as could be detected in spleen and lymph nodes. However the deletion rates in these organs were lower than in the thymus, indicating a developmental advantage of the few thymocytes escaping UBPY deletion. The mice were viable and exhibited no obvious phenotypical changes until the age of around six weeks, after which they started to develop a lethal colitis, which will be discussed later. The UBPYΔ^{T} mice are the first T cell-specific knockout mouse model for a ubiquitin-specific protease. These mice represent a convenient tool for the study of UBPY function *in vivo* and *ex vivo*. They allowed to study the impact of UBPY deletion on the immune system and, since UBPY deletion already starts at the T cell precursor stage, on thymocyte development. These mice were also a suitable source of UBPY depleted primary cells (thymocytes) permitting the study of endosomal trafficking by tracing TCR levels. The UBPYΔ^{T} animals also enabled to determine a previously undescribed role of UBPY in TCR signal transduction.

6.2 The role of UBPY in T cell development

Thymocyte development proceeds through three main stages at which signal transduction through the pre-T-cell-receptor (pre-TCR) or through the mature $\alpha\beta$TCR is required (reviewed in [91]).

The first signaling checkpoint takes place at the DN3 stage of development. Thymocytes that have successfully rearranged the TCRβ chain express the pre-TCR composed of the TCRβ chain together with the invariant pre-Tα polypeptide. Effective pre-TCR signaling induces allelic exclusion of the TCRβ locus, thus inhibiting further recombination events, followed by a brief period of strong proliferation leading to expansion of the T cell bearing the functional TCRβ chain. Also, CD4 and CD8 coreceptor expression is initiated. Before entering the DP stage, cells stop to proliferate and enter a cell cycle arrest enabling rearrangement of the TCRα chain. Patterns of CD44 and CD25 surface expression in UBPYΔ^T DN thymocytes were unaltered and the frequencies and total numbers of DP thymocytes were similar in UBPYΔ^T and wildtype animals. Only the CD5 expression in DN thymocytes was slightly reduced in UBPYΔ^T mice(Fig.5.4). Southern Blot analysis showed that in DN thymocytes from UBPYΔ^T mice the floxed UBPY allele is already deleted in a fraction of the cells(Fig.5.1). The effect on CD5 expression could be due to a starting reduction of UBPY protein levels interfering with ongoing pre-TCR signaling. Even so, the levels of UBPY in DN thymocytes of UBPYΔ^T mice are obviously sufficient for their normal expansion and differentiation to DP thymocytes.

The second signaling checkpoint occurs at the DP stage of thymocyte development. The DP thymocytes rearrange the TCRα chain and express a mature $\alpha\beta$TCR at their surface. In the thymic cortex, the thymocytes move around until they find a self-peptide MHC complex on which they can be positively selected. Lack of binding leads to death by neglect. After positive selection the thymocytes differentiate into single positive thymocytes and migrate to the thymic medulla, where they again encounter self-peptide MHC complexes, this time presented by medullary thymic epithelial cells (mTEC), specialized for central tolerance. High affinity interaction with these complexes leads to clonal deletion or alternatively to positive selection of regulatory cells. While frequencies and numbers of DN and DP thymocytes in UBPYΔ^T were

unchanged, both CD4 and CD8 SP thymocyte populations were drastically reduced. The remaining CD4 and CD8 SP cells displayed immature surface phenotypes, with lower expression of CD3ϵ, CD5 and CD69, markers typically upregulated after positive selection. The most mature thymocytes, with low to absent expression of HSA, were almost absent in UBPYΔ^T mice. After positive selection, the thymocytes undergo activation and cellular proliferation. Since several publications reported a growth arrest in cells depleted of UBPY [8, 9], it was likely that positive selection in UBPYΔ^T mice was impaired due to a proliferation defect. However, BrdU incorporation experiments *in vivo* showed that the percentages of proliferating cells within the different UBPYΔ^T thymocyte subsets were not reduced, thus demonstrating that UBPY is not required for cell cycle progression in thymocytes. *In vitro*, though, proliferation of thymocytes in response to TCR stimulation was impaired, unless exogenous interleukin-2 was added to the medium. An increased susceptibility to apoptosis after TCR stimulation *in vitro* could not be detected. However, since even in wildtype cells less then 10% of the cells remained viable after 48h of culture, this test might not be suitable to detect differences in apoptosis induction after longer incubation periods. UBPYΔ^T thymocytes also failed to produce interleukin-2 in response to TCR stimulation. Thus, these results showed a defective responsiveness of UBPYΔ^T thymocytes to TCR stimulation, which could be caused by a decreased viability or susceptibility of the thymocytes after longer periods of incubation. These results do not allow a conclusion on defects in positive and/or negative selection in UBPYΔ^T mice. Further studies using mice transgenic for the H-Y TCR will be needed to answer this.

Molecular analysis of the signal transduction events in UBPYΔ^T thymocytes showed that signals through the TCR are transmitted, but display altered kinetics. ERK phosphorylation was stronger at early timepoints but more transient. Recent evidence indicates that beside the strength of the signal transmitted through the TCR also the duration of the signal are crucial factors both for the decision between positive versus negative selection as for lineage commitment (reviewed in

[92]). While negative selecting ligands induce are stronger, but more transient signal,as measured by ERK phosphorylation, positive selecting ligands induce a weaker but more sustained ERK phosphorylation. Similarily lineage commitment seems to be dependent of the kinetics in TCR signaling, with development of CD4 SP thymocytes requiring stronger and/or longer signals. In UBPYΔ^T thymocytes the development of CD4SP thymocytes is more severely affected than the development of CD8SP thymocytes, in terms of frequencies and numbers. Rather than an abrogation of TCR signaling, a defect in mounting a sustained ERK signal in UBPYΔ^T thymocytes could underlie both the defective positive selection and the alterations in lineage commitment observed in UBPYΔ^T mice.

How could UBPY possibly regulate TCR signal kinetics? First, we tested if lack of deubiquitination by UBPY would lead to a destabilization of certain components of the TCR signaling machinery or of certain E3 ligases, but for none of the molecules tested an increased degradation could be detected. There is increasing evidence that ubiquitination can regulate TCR signaling in a degradation-independent way. Ubiquitination of the p85 subunit of Phosphatidyl-inositol 3 kinase (PI3K) by cbl-b for example was reported to prevent its recruitment to CD28 and TCRζ, without affecting its stability [59]. Also negative regulation of TCR signaling through ubiquitination of PLC-γ and Lck was argued to be a proteolysis-independent mechanism [55, 93]. In c-cbl/cbl-b double-knockout mice, a defect in ligand-induced TCR downmodulation leads to prolonged TCR signaling and hyperresponsiveness in mature T cells [69]. It was therefore easily conceivable, that, conversely, increased TCR downmodulation could cause the shortened TCR signals in UBPY deficient thymocytes. However we could not detect any aberrations in the regulation of TCRβ surface levels neither with nor without stimulation. This result clearly shows that UBPY is not involved in intracellular trafficking of the TCR. In addition to this result, we could not detect an accumulation of ubiquitinated susbtrates [10, 11, 9], nor could we detect a reduction in the levels of Hrs and STAM as described in previous studies of UBPY depletion. Thus,

endosomal trafficking of ubiquitinated substrates seems not to be globally affected in UBPYΔ^T thymocytes.

Other than the TCR, intracellular localization of several TCR signaling molecules may influence TCR signaling outcome. A recent study proposed that selection outcome in thymocytes is dependent on subcellular localization of several components of the Ras/ERK pathway [75]. Negative selecting ligands induced a strong and transient ERK phosphorylation, and phosphorylated ERK was preferentially targeted to the plasma membrane. Positive selecting ligands instead induced less ERK phosphorylation more slowly, and phosphorylated ERK accumulated throughout the cell. Similar localization patterns were observed for other members of the pathway such as Ras, Raf-1, Grb-2 and SOS. Differential ubiquitination has been shown to regulate compartmentalized signaling of Ras, with ubiquitinated HRas preferentially associating with endosomes [94]. Deregulation of Ras/MAPK compartmentalization could therefore represent a plausible explanation for the aberrations observed in UBPY-deficient thymocytes, embracing the previously described functions of UBPY in endosomal trafficking and cell growth. Future work will be needed to address this issue.

6.3 The role of UBPY in T cell homeostasis and function

UBPY-deficient mice have defects in T cell homeostasis and function that are manifested by decreased frequencies of naïve and increased frequencies of effector T cell subsets and development of spontaneous colitis.

Colitis is caused by an imbalance between effector and regulatory T cell responses, shifting the homeostasis of the mucosal immune system towards inflammation [76]. As depicted in Figure 6.1, this imbalance can result from either a particularly robust effector response or a weakened

regulatory response.

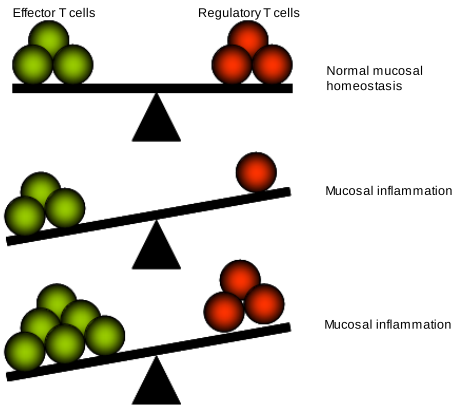

Figure 6.1: Pathways to mucosal inflammation. Normal mucosal homeostasis is maintained by a delicate balance of effector (green circles) and regulatory (red circles) T cells (upper panel). Disturbance of this balance by impaired regulatory T cell function (middle panel) or, alternatively, by excessive responses of effector T cells despite normal regulatory T cell function (lower panel) leads to mucosal inflammation.

Analysis of young UBPYΔ^T mice, before onset of disease showed that the peripheral T cells are aberrantly high activated and mostly display an effector phenotype, while naïve and memory T cells were nearly absent.

This is in sharp contrast to the defective responsiveness of thymocytes in UBPYΔ^T mice, but at a closer view not necessarily contradictory. Under normal conditions, TCR signals transmitted in a thymocyte reflect the affinity/avidity of its TCR to MHC-self antigen complexes and trigger the appropriate selection process. However, in UBPYΔ^T thymocyte development is impaired, with defects in thymocyte selection probably caused by aberrant TCR signaling. This might alter selection outcome and lead to positive selection of hyperreactive T cells.
UBPYΔ^T thymocytes were not able to proliferate and to produce interleukin-2 in response to TCR stimulation. It is therefore puzzling at first, how any UBPY deleted T cells could appear in the periphery. Two results might contribute to the answer. First, the mature T cell compartment in UBPYΔ^T mice was only partly composed of UBPY-deficient cells and contained a large fraction cells with the non-recombined UBPY allele, probably due to leaky cre expression in

these cells. Second, proliferation in UBPY-depleted thymocytes could be restored by addition of recombinant Interleukin-2 in the medium. Proliferation and maturation of the UBPY-depleted T cells was therefore likely made possible by the interleukin-2 produced by the wildtype cells.

Knockout of the deubiquitinating enzyme CYLD (cylindromatosis gene product), leads to a similar defect in thymic development [55] as in UBPYΔ^T mice and to development of colitis due to hyperresponsive peripheral T cells [56]. The group explained this by divergent functions of CYLD in thymocytes and mature T cells. Similiarily, UBPY could have a specific function in mature T cells. So, UBPY was proposed to stabilize GRAIL, an E3 ligase necessary for anergy induction [13]. Lack of UBPY in peripheral T cells could therefore interfere with anergy induction as a mechanism of peripheral tolerance.

GRAIL was also shown to be involved in induction of regulatory T cells [95]. We could not detect decreased levels of GRAIL in UBPYΔ^T total thymocyte extracts, showing that UBPY is not required for maintenance of constitutive levels of GRAIL in thymocytes. Stabilization of GRAIL by UBPY might only be needed for the upregulation of the E3 ligase in regulatory T cells and in mature T cells after anergy induction [96]. Regulatory T cells derive from the thymus and are positively selected through a high-affinity recognition of self-peptides presented by thymic stromal cells [97]. In UBPYΔ^T mice, total numbers of CD4+CD25+ regulatory T cells were also reduced. However, instead of the total number, the percentage of CD4+CD25^{high} relative to total CD4+ cells should be taken into account for the evaluation of the regulatory T cell compartment and this frequency is unaltered in UBPYΔ^T mice. Again, the aberrations in TCR signaling might alter outcome of regulatory T cell selection.

UBPYΔ^T mice exhibited a hyperactivation of peripheral T cells prior to onset of the disease. In addition, they had defects in thymocyte selection and lymphopenia resulting from decreased thymic output. A combination of these abnormalities is likely to contribute to the development of colitis in UBPY mice. However, the present state of work does not allow a definitive conclusion

on this point. Future work should involve *ex vivo* testing of the responsiveness of naïve T cells from UBPYΔ^T mice to TCR stimulation. Also, defects in regulatory T cell function should be assessed by transfer experiments.

Summary

Mono- and polyubiquitination controls a multitude of cellular processes beside proteasomal degradation, including the activity of signaling cascades, DNA replication and repair, subcellular localization of proteins and virus budding [20]. The reversibility of ubiquitination is ensured by a large group of deubiquitinating enzymes with important regulatory functions [5, 22].

The ubiquitin specific peptidase UBPY has a vital and non-redundant role, demonstrated by the fact that the conventional knockout of UBPY is embryonically lethal [9]. Further studies revealed a function of UBPY in endocytic trafficking and in ligand-induced downmodulation of receptor tyrosine kinases [10, 11, 9]. Both mechanisms play a central role in T cell development and function. UBPY was also reported to interact with a major player in TCR signaling, the adaptor molecule GADS [12], and with a central regulator of T cell anergy, the E3 ligase GRAIL [13].

To investigate the T cell specific functions of UBPY, cre/LoxP targeting was used to generate a knockout mouse model lacking UBPY exclusively in T cells (UBPYΔ^T).

UBPYΔ^T mice have defects in immune homeostasis, causing hyperactivation of the peripheral T cells, the spontaneous development of inflammatory bowel disease and premature death of the animals. This phenotype probably underlies a defective thymocyte development in UBPYΔ^T mice leading to reduced levels of single positive thymocytes and of mature T cells. UBPY, however, is not necessary for normal proliferation of thymocytes and not for endosomal trafficking of the TCR. Rather, UBPY depletion alters TCR signal transduction, leading to stronger but more transient ERK phosphorylation after TCR stimulation. This work could thus determine a previously undescribed function of a deubiquitinating enzyme in the regulation of TCR signal kinetics, with potential importance for other signal transduction pathways.

Zusammenfassung

Mono- und Polyubiquitinierung reguliert eine Vielzahl von zellulären Prozessen neben der proteasomalen Degradation, die von der Aktivität von Signaltransduktionskaskaden, über DNA Replikation und Reparatur, subzellulärer Lokalisation von Proteinen bis zur Knospung (Budding) von Viruspartikeln reichen[20]. Die Umkehrbarkeit der Ubiquitinierung wird dabei durch eine ausgedehnte Gruppe von deubiquitinierenden Enzymen mit bedeutenden regulatorischen Funktionen gewährleistet [5, 22].

Die Ubiquitin spezifische Peptidase UBPY erfüllt eine essentielle und nicht-redundante Rolle, was anhand des embryonal lethalen Phenotyp des konventionellen Knockouts von UBPY [9] ersichtlich wird. Weiters wurde eine Funktion der Isopeptidase im endosomalen Transport (trafficking) und in der Liganden-vermittelten Herabregulierung von Rezeptortyrosinkinasen [10, 11, 9] gezeigt. Beide Mechanismen sind wesentlich für die Entwicklung und Funktion von T-Zellen. Zudem wurde gezeigt, dass UBPY mit einem wichtigen Adaptormolekül des T-Zell-Rezeptor (TZR)-Signalwegs interagiert, GADS [12], sowie mit einem zentralen Steuerelement der T-Zell-Anergie, der E3 Ligase GRAIL [13].

Um daher die T-Zell-spezifischen Funktionen von UBPY zu analysieren, wurde mittels cre/LoxP targeting ein Mausmodell generiert, in dem UBPY ausschliesslich in T-Zellen ausgeschaltet ist (UBPYΔ^T).

Die UBPYΔ^T Mäuse haben ein defektes Immungleichgewicht, welches sich in der Überaktivierung der periphären T-Zellen und der spontanen Entwicklung einer entzündlichen Darmerkrankung manifestiert und zu einem vorzeitigen Tod der Tiere führt. Diesem Phänotyp dürfte die gestörte Thymozytenentwicklung in UBPYΔ^T Mäusen zugrundeliegen, die zu einer Verminderung der einfach positiven (single positive) Thymozyten und der reifen T Zellen führt. UBPY ist nicht notwendig für die Proliferation von T Zellen und steuert nicht den Transport des TZR im Endozy-

toseweg. UBPY Depletion führt hingegen zu einer stärkeren aber verkürzten ERK-Phosphorylierung nach Stimulation durch den TZR. Diese Arbeit konnte daher eine bisher noch nicht beschriebene Funktion eines Deubiquitinierungsenzyms in der Regulation der Kinetik von TZR-vermittelten Signalen zeigen, die auch in anderen Signalwegen eine bedeutende Rolle spielen könnte.

Bibliography

[1] A. Ciechanover, H. Heller, S. Elias, A. L. Haas, and A. Hershko. ATP-dependent conjugation of reticulocyte proteins with the polypeptide required for protein degradation. *Proc Natl Acad Sci U S A*, 77(3):1365–1368, Mar 1980.

[2] A. Hershko, A. Ciechanover, H. Heller, A. L. Haas, and I. A. Rose. Proposed role of ATP in protein breakdown: conjugation of protein with multiple chains of the polypeptide of ATP-dependent proteolysis. *Proc Natl Acad Sci U S A*, 77(4):1783–1786, Apr 1980.

[3] M. Glotzer, A. W. Murray, and M. W. Kirschner. Cyclin is degraded by the ubiquitin pathway. *Nature*, 349(6305):132–138, Jan 1991.

[4] T. Rinaldi, C. Ricci, D. Porro, M. Bolotin-Fukuhara, and L. Frontali. A mutation in a novel yeast proteasomal gene, rpn11/mpr1, produces a cell cycle arrest, overreplication of nuclear and mitochondrial dna, and an altered mitochondrial morphology. *Mol Biol Cell*, 9(10):2917–2931, Oct 1998.

[5] Alexander Y Amerik and Mark Hochstrasser. Mechanism and function of deubiquitinating enzymes. *Biochim Biophys Acta*, 1695(1-3):189–207, Nov 2004.

[6] David L Boone, Emre E Turer, Eric G Lee, Regina-Celeste Ahmad, Matthew T Wheeler, Colleen Tsui, Paula Hurley, Marcia Chien, Sophia Chai, Osamu Hitotsumatsu, Elizabeth McNally, Cecile Pickart, and Averil Ma. The ubiquitin-modifying enzyme A20 is required for termination of toll-like receptor responses. *Nat Immunol*, 5(10):1052–1060, Oct 2004.

[7] Sarika Saggar, Karen A Chernoff, Saurabh Lodha, Liran Horev, Shane Kohl, Rachel Honjo, Hebert Brandt, Karin Hartman, and Julide Tok Celebi. Cyld mutations in familial skin appendage tumors. *J Med Genet*, Feb 2008.

[8] S. Naviglio, C. Mattecucci, B. Matoskova, T. Nagase, N. Nomura, P. P. Di Fiore, and G. F. Draetta. UBPY: a growth-regulated human ubiquitin isopeptidase. *EMBO J*, 17(12):3241–3250, Jun 1998.

[9] Sandra Niendorf, Alexander Oksche, Agnes Kisser, Jürgen Löhler, Marco Prinz, Hubert Schorle, Stephan Feller, Marc Lewitzky, Ivan Horak, and Klaus-Peter Knobeloch. Essential role of ubiquitin-specific protease 8 for receptor tyrosine kinase stability and endocytic trafficking in vivo. *Mol Cell Biol*, 27(13):5029–5039, Jul 2007.

[10] Paula E Row, Ian A Prior, John McCullough, Michael J Clague, and Sylvie Urbé. The ubiquitin isopeptidase UBPY regulates endosomal ubiquitin dynamics and is essential for receptor down-regulation. *J Biol Chem*, 281(18):12618–12624, May 2006.

[11] Emi Mizuno, Kaoru Kobayashi, Akitsugu Yamamoto, Naomi Kitamura, and Masayuki Komada. A deubiquitinating enzyme UBPY regulates the level of protein ubiquitination on endosomes. *Traffic*, 7(8):1017–1031, Aug 2006.

[12] Marc Lewitzky. *Signalling through small SH2/SH3 adaptor proteins of the Grb2 family*. PhD thesis, Faculty of Clinical Medicine at the University of Oxford, 2005.

[13] Luis Soares, Christine Seroogy, Heidi Skrenta, Niroshana Anandasabapathy, Patricia Lovelace, Chan D Chung, Edgar Engleman, and C. Garrison Fathman. Two isoforms of otubain 1 regulate T cell anergy via GRAIL. *Nat Immunol*, 5(1):45–54, Jan 2004.

[14] Linton M Traub and Gergely L Lukacs. Decoding ubiquitin sorting signals for clathrin-dependent endocytosis by CLASPs. *J Cell Sci*, 120(Pt 4):543–553, Feb 2007.

[15] Michael H Glickman and Aaron Ciechanover. The ubiquitin-proteasome proteolytic pathway: destruction for the sake of construction. *Physiol Rev*, 82(2):373–428, Apr 2002.

[16] Marcus Groettrup, Christiane Pelzer, Gunter Schmidtke, and Kay Hofmann. Activating the ubiquitin family: Uba6 challenges the field. *Trends Biochem Sci*, Mar 2008.

[17] Cecile M Pickart. Back to the future with ubiquitin. *Cell*, 116(2):181–190, Jan 2004.

[18] Christoph Berndt, Dawadschargal Bech-Otschir, Wolfgang Dubiel, and Michael Seeger. Ubiquitin system: JAMMing in the name of the lid. *Curr Biol*, 12(23):R815–R817, Dec 2002.

[19] Robert C Piper and J. Paul Luzio. Ubiquitin-dependent sorting of integral membrane proteins for degradation in lysosomes. *Curr Opin Cell Biol*, 19(4):459–465, Aug 2007.

[20] Linda Hicke and Rebecca Dunn. Regulation of membrane protein transport by ubiquitin and ubiquitin-binding proteins. *Annu Rev Cell Dev Biol*, 19:141–172, 2003.

[21] Roger L Williams and Sylvie Urbé. The emerging shape of the ESCRT machinery. *Nat Rev Mol Cell Biol*, 8(5):355–368, May 2007.

[22] Sebastian M B Nijman, Mark P A Luna-Vargas, Arno Velds, Thijn R Brummelkamp, Annette M G Dirac, Titia K Sixma, and René Bernards. A genomic and functional inventory of deubiquitinating enzymes. *Cell*, 123(5):773–786, Dec 2005.

[23] Colin A M Semple, R. I. K. E. N. GER Group, and G. S. L. Members. The comparative proteomics of ubiquitination in mouse. *Genome Res*, 13(6B):1389–1394, Jun 2003.

[24] K. S. Makarova, L. Aravind, and E. V. Koonin. A novel superfamily of predicted cysteine proteases from eukaryotes, viruses and Chlamydia pneumoniae. *Trends Biochem Sci*, 25(2):50–52, Feb 2000.

[25] Max H Nanao, Sergey O Tcherniuk, Jadwiga Chroboczek, Otto Dideberg, Andréa Dessen, and Maxim Y Balakirev. Crystal structure of human otubain 2. *EMBO Rep*, 5(8):783–788, Aug 2004.

[26] Ingrid E Wertz, Karen M O'Rourke, Honglin Zhou, Michael Eby, L. Aravind, Somasekar Seshagiri, Ping Wu, Christian Wiesmann, Rohan Baker, David L Boone, Averil Ma, Eugene V Koonin, and Vishva M Dixit. De-ubiquitination and ubiquitin ligase domains of a20 downregulate nf-kappab signalling. *Nature*, 430(7000):694–699, Aug 2004.

[27] Nobuhiko Kayagaki, Qui Phung, Salina Chan, Ruchir Chaudhari, Casey Quan, Karen M O'Rourke, Michael Eby, Eric Pietras, Genhong Cheng, J. Fernando Bazan, Zemin Zhang, David Arnott, and Vishva M Dixit. DUBA: a deubiquitinase that regulates type I interferon production. *Science*, 318(5856):1628–1632, Dec 2007.

[28] Hartmut Scheel, Stefan Tomiuk, and Kay Hofmann. Elucidation of ataxin-3 and ataxin-7 function by integrative bioinformatics. *Hum Mol Genet*, 12(21):2845–2852, Nov 2003.

[29] Mark Hochstrasser. Molecular biology. New proteases in a ubiquitin stew. *Science*, 298(5593):549–552, Oct 2002.

[30] Xavier I Ambroggio, Douglas C Rees, and Raymond J Deshaies. JAMM: a metalloprotease-like zinc site in the proteasome and signalosome. *PLoS Biol*, 2(1):E2, Jan 2004.

[31] S. Urbé, J. McCullough, P. Row, I. A. Prior, R. Welchman, and M. J. Clague. Control of growth factor receptor dynamics by reversible ubiquitination. *Biochem Soc Trans*, 34(Pt 5):754–756, Nov 2006.

[32] M. Hochstrasser. Ubiquitin-dependent protein degradation. *Annu Rev Genet*, 30:405–439, 1996.

[33] P. K. Lund, B. M. Moats-Staats, J. G. Simmons, E. Hoyt, A. J. D'Ercole, F. Martin, and J. J. Van Wyk. Nucleotide sequence analysis of a cDNA encoding human ubiquitin reveals that ubiquitin is synthesized as a precursor. *J Biol Chem*, 260(12):7609–7613, Jun 1985.

[34] J. S. Thrower, L. Hoffman, M. Rechsteiner, and C. M. Pickart. Recognition of the polyubiquitin proteolytic signal. *EMBO J*, 19(1):94–102, Jan 2000.

[35] Elena Koulich, Xiaohua Li, and George N Demartino. Relative structural and functional roles of multiple deubiquitylating proteins associated with mammalian 26s proteasome. *Mol Biol Cell*, 19(3):1072–1082, Mar 2008.

[36] K. D. Wilkinson, V. L. Tashayev, L. B. O'Connor, C. N. Larsen, E. Kasperek, and C. M. Pickart. Metabolism of the polyubiquitin degradation signal: structure, mechanism, and role of isopeptidase T. *Biochemistry*, 34(44):14535–14546, Nov 1995.

[37] S. Swaminathan, A. Y. Amerik, and M. Hochstrasser. The doa4 deubiquitinating enzyme is required for ubiquitin homeostasis in yeast. *Mol Biol Cell*, 10(8):2583–2594, Aug 1999.

[38] N. Gnesutta, M. Ceriani, M. Innocenti, I. Mauri, R. Zippel, E. Sturani, B. Borgonovo, G. Berruti, and E. Martegani. Cloning and characterization of mouse UBPy, a deubiquitinating enzyme that interacts with the ras guanine nucleotide exchange factor CDC25(Mm)/Ras-GRF1. *J Biol Chem*, 276(42):39448–39454, Oct 2001.

[39] Paula E Row, Han Liu, Sebastian Hayes, Rebecca Welchman, Panagoula Charalabous, Kay Hofmann, Michael J Clague, Christopher M Sanderson, and Sylvie Urbé. The MIT domain

of UBPY constitutes a CHMP binding and endosomal localization signal required for efficient epidermal growth factor receptor degradation. *J Biol Chem*, 282(42):30929–30937, Oct 2007.

[40] Emi Mizuno, Takanobu Iura, Akiko Mukai, Tamotsu Yoshimori, Naomi Kitamura, and Masayuki Komada. Regulation of epidermal growth factor receptor down-regulation by UBPY-mediated deubiquitination at endosomes. *Mol Biol Cell*, 16(11):5163–5174, Nov 2005.

[41] Xiuli Wu, Lily Yen, Lisa Irwin, Colleen Sweeney, and Kermit L Carraway. Stabilization of the E3 ubiquitin ligase Nrdp1 by the deubiquitinating enzyme USP8. *Mol Cell Biol*, 24(17):7748–7757, Sep 2004.

[42] M. Kato, K. Miyazawa, and N. Kitamura. A deubiquitinating enzyme UBPY interacts with the Src homology 3 domain of Hrs-binding protein via a novel binding motif PX(V/I)(D/N)RXXKP. *J Biol Chem*, 275(48):37481–37487, Dec 2000.

[43] Lawrence E Samelson. Signal transduction mediated by the T cell antigen receptor: the role of adapter proteins. *Annu Rev Immunol*, 20:371–394, 2002.

[44] Bryan A Ballif, Zhongwei Cao, Daniel Schwartz, Kermit L Carraway, and Steven P Gygi. Identification of 14-3-3epsilon substrates from embryonic murine brain. *J Proteome Res*, 5(9):2372–2379, Sep 2006.

[45] Sarah E M Meek, William S Lane, and Helen Piwnica-Worms. Comprehensive proteomic analysis of interphase and mitotic 14-3-3-binding proteins. *J Biol Chem*, 279(31):32046–32054, Jul 2004.

[46] Anne Benzinger, Nemone Muster, Heike B Koch, John R Yates, and Heiko Hermeking. Targeted proteomic analysis of 14-3-3 sigma, a p53 effector commonly silenced in cancer. *Mol Cell Proteomics*, 4(6):785–795, Jun 2005.

[47] Heiko Hermeking and Anne Benzinger. 14-3-3 proteins in cell cycle regulation. *Semin Cancer Biol*, 16(3):183–192, Jun 2006.

[48] Emi Mizuno, Naomi Kitamura, and Masayuki Komada. 14-3-3-dependent inhibition of the deubiquitinating activity of UBPY and its cancellation in the M phase. *Exp Cell Res*, 313(16):3624–3634, Oct 2007.

[49] Katherine Bowers, Siân C Piper, Melissa A Edeling, Sally R Gray, David J Owen, Paul J Lehner, and J. Paul Luzio. Degradation of endocytosed epidermal growth factor and virally ubiquitinated major histocompatibility complex class I is independent of mammalian ESCRTII. *J Biol Chem*, 281(8):5094–5105, Feb 2006.

[50] Husam A J Alwan and Jeroen E M van Leeuwen. UBPY-mediated epidermal growth factor receptor (EGFR) de-ubiquitination promotes EGFR degradation. *J Biol Chem*, 282(3):1658–1669, Jan 2007.

[51] C. M. Pickart. Ubiquitin enters the new millennium. *Mol Cell*, 8(3):499–504, Sep 2001.

[52] Yun-Cai Liu, Josef Penninger, and Michael Karin. Immunity by ubiquitylation: a reversible process of modification. *Nat Rev Immunol*, 5(12):941–952, Dec 2005.

[53] M. Naramura, H. K. Kole, R. J. Hu, and H. Gu. Altered thymic positive selection and intracellular signals in Cbl-deficient mice. *Proc Natl Acad Sci U S A*, 95(26):15547–15552, Dec 1998.

[54] M. A. Murphy, R. G. Schnall, D. J. Venter, L. Barnett, I. Bertoncello, C. B. Thien, W. Y. Langdon, and D. D. Bowtell. Tissue hyperplasia and enhanced t-cell signalling via zap-70 in c-cbl-deficient mice. *Mol Cell Biol*, 18(8):4872–4882, Aug 1998.

[55] William W Reiley, Minying Zhang, Wei Jin, Mandy Losiewicz, Keri B Donohue, Christopher C Norbury, and Shao-Cong Sun. Regulation of T cell development by the deubiquitinating enzyme CYLD. *Nat Immunol*, 7(4):411–417, Apr 2006.

[56] William W Reiley, Wei Jin, Andrew Joon Lee, Ato Wright, Xuefeng Wu, Eric F Tewalt, Timothy O Leonard, Christopher C Norbury, Leo Fitzpatrick, Minying Zhang, and Shao-Cong Sun. Deubiquitinating enzyme cyld negatively regulates the ubiquitin-dependent kinase tak1 and prevents abnormal t cell responses. *J Exp Med*, 204(6):1475–1485, Jun 2007.

[57] Ronald H Schwartz. T cell anergy. *Annu Rev Immunol*, 21:305–334, 2003.

[58] V. A. Boussiotis, G. J. Freeman, A. Berezovskaya, D. L. Barber, and L. M. Nadler. Maintenance of human T cell anergy: blocking of IL-2 gene transcription by activated Rap1. *Science*, 278(5335):124–128, Oct 1997.

[59] D. Fang and Y. C. Liu. Proteolysis-independent regulation of PI3K by Cbl-b-mediated ubiquitination in T cells. *Nat Immunol*, 2(9):870–875, Sep 2001.

[60] Y. J. Chiang, H. K. Kole, K. Brown, M. Naramura, S. Fukuhara, R. J. Hu, I. K. Jang, J. S. Gutkind, E. Shevach, and H. Gu. Cbl-b regulates the CD28 dependence of T-cell activation. *Nature*, 403(6766):216–220, Jan 2000.

[61] K. Bachmaier, C. Krawczyk, I. Kozieradzki, Y. Y. Kong, T. Sasaki, A. Oliveira dos Santos, S. Mariathasan, D. Bouchard, A. Wakeham, A. Itie, J. Le, P. S. Ohashi, I. Sarosi, H. Nishina, S. Lipkowitz, and J. M. Penninger. Negative regulation of lymphocyte activation and autoimmunity by the molecular adaptor Cbl-b. *Nature*, 403(6766):211–216, Jan 2000.

[62] Vigo Heissmeyer and Anjana Rao. E3 ligases in T cell anergy–turning immune responses into tolerance. *Sci STKE*, 2004(241):pe29, Jul 2004.

[63] Deyu Fang, Chris Elly, Baixue Gao, Nan Fang, Yoav Altman, Claudio Joazeiro, Tony Hunter, Neal Copeland, Nancy Jenkins, and Yun-Cai Liu. Dysregulation of T lymphocyte function in itchy mice: a role for Itch in TH2 differentiation. *Nat Immunol*, 3(3):281–287, Mar 2002.

[64] H. Liu, M. Rhodes, D. L. Wiest, and D. A. Vignali. On the dynamics of TCR:CD3 complex cell surface expression and downmodulation. *Immunity*, 13(5):665–675, Nov 2000.

[65] S. Valitutti, S. Müller, M. Salio, and A. Lanzavecchia. Degradation of T cell receptor (TCR)-CD3-zeta complexes after antigenic stimulation. *J Exp Med*, 185(10):1859–1864, May 1997.

[66] Michal Baniyash. TCR zeta-chain downregulation: curtailing an excessive inflammatory immune response. *Nat Rev Immunol*, 4(9):675–687, Sep 2004.

[67] H. Y. Wang, Y. Altman, D. Fang, C. Elly, Y. Dai, Y. Shao, and Y. C. Liu. Cbl promotes ubiquitination of the T cell receptor zeta through an adaptor function of Zap-70. *J Biol Chem*, 276(28):26004–26011, Jul 2001.

[68] Margaret D Myers, Tomasz Sosinowski, Leonard L Dragone, Carmen White, Hamid Band, Hua Gu, and Arthur Weiss. Src-like adaptor protein regulates TCR expression on thymocytes by linking the ubiquitin ligase c-Cbl to the TCR complex. *Nat Immunol*, 7(1):57–66, Jan 2006.

[69] Mayumi Naramura, Ihn-Kyung Jang, Hemanta Kole, Fang Huang, Diana Haines, and Hua Gu. c-Cbl and Cbl-b regulate T cell responsiveness by promoting ligand-induced TCR down-modulation. *Nat Immunol*, 3(12):1192–1199, Dec 2002.

[70] W. L. Havran, M. Poenie, J. Kimura, R. Tsien, A. Weiss, and J. P. Allison. Expression and function of the CD3-antigen receptor on murine CD4+8+ thymocytes. *Nature*, 330(6144):170–173, 1987.

[71] Jun Zhang, Brigid Stirling, Stephane T Temmerman, Chi A Ma, Ivan J Fuss, Jonathan M J Derry, and Ashish Jain. Impaired regulation of nf-kappab and increased susceptibility to colitis-associated tumorigenesis in cyld-deficient mice. *J Clin Invest*, 116(11):3042–3049, Nov 2006.

[72] Thijn R Brummelkamp, Sebastian M B Nijman, Annette M G Dirac, and René Bernards. Loss of the cylindromatosis tumour suppressor inhibits apoptosis by activating nf-kappab. *Nature*, 424(6950):797–801, Aug 2003.

[73] Andrew Kovalenko, Christine Chable-Bessia, Giuseppina Cantarella, Alain Israël, David Wallach, and Gilles Courtois. The tumour suppressor cyld negatively regulates nf-kappab signalling by deubiquitination. *Nature*, 424(6950):801–805, Aug 2003.

[74] Eirini Trompouki, Eudoxia Hatzivassiliou, Theodore Tsichritzis, Hannah Farmer, Alan Ashworth, and George Mosialos. Cyld is a deubiquitinating enzyme that negatively regulates nf-kappab activation by tnfr family members. *Nature*, 424(6950):793–796, Aug 2003.

[75] Mark A Daniels, Emma Teixeiro, Jason Gill, Barbara Hausmann, Dominique Roubaty, Kaisa Holmberg, Guy Werlen, Georg A Holländer, Nicholas R J Gascoigne, and Ed Palmer. Thymic selection threshold defined by compartmentalization of ras/mapk signalling. *Nature*, 444(7120):724–729, Dec 2006.

[76] Gerd Bouma and Warren Strober. The immunological and genetic basis of inflammatory bowel disease. *Nat Rev Immunol*, 3(7):521–533, Jul 2003.

[77] D. Kontoyiannis, M. Pasparakis, T. T. Pizarro, F. Cominelli, and G. Kollias. Impaired on/off regulation of TNF biosynthesis in mice lacking TNF AU-rich elements: implications for joint and gut-associated immunopathologies. *Immunity*, 10(3):387–398, Mar 1999.

[78] S. Wirtz, S. Finotto, S. Kanzler, A. W. Lohse, M. Blessing, H. A. Lehr, P. R. Galle, and M. F. Neurath. Cutting edge: chronic intestinal inflammation in STAT-4 transgenic mice: characterization of disease and adoptive transfer by TNF- plus IFN-gamma-producing CD4+ T cells that respond to bacterial antigens. *J Immunol*, 162(4):1884–1888, Feb 1999.

[79] C. Asseman, S. Mauze, M. W. Leach, R. L. Coffman, and F. Powrie. An essential role for interleukin 10 in the function of regulatory T cells that inhibit intestinal inflammation. *J Exp Med*, 190(7):995–1004, Oct 1999.

[80] B. Sadlack, H. Merz, H. Schorle, A. Schimpl, A. C. Feller, and I. Horak. Ulcerative colitis-like disease in mice with a disrupted interleukin-2 gene. *Cell*, 75(2):253–261, Oct 1993.

[81] H. S. Azzam, A. Grinberg, K. Lui, H. Shen, E. W. Shores, and P. E. Love. CD5 expression is developmentally regulated by T cell receptor (TCR) signals and TCR avidity. *J Exp Med*, 188(12):2301–2311, Dec 1998.

[82] G. Anderson, K. J. Hare, and E. J. Jenkinson. Positive selection of thymocytes: the long and winding road. *Immunol Today*, 20(10):463–468, Oct 1999.

[83] Weifeng Chen. The late stage of T cell development within mouse thymus. *Cell Mol Immunol*, 1(1):3–11, Feb 2004.

[84] A. Tarakhovsky, W. Müller, and K. Rajewsky. Lymphocyte populations and immune responses in CD5-deficient mice. *Eur J Immunol*, 24(7):1678–1684, Jul 1994.

[85] M. Lenardo, K. M. Chan, F. Hornung, H. McFarland, R. Siegel, J. Wang, and L. Zheng. Mature t lymphocyte apoptosis–immune regulation in a dynamic and unpredictable antigenic environment. *Annu Rev Immunol*, 17:221–253, 1999.

[86] M. A. Nieto, A. González, A. López-Rivas, F. Diaz-Espada, and F. Gambón. Il-2 protects against anti-cd3-induced cell death in human medullary thymocytes. *J Immunol*, 145(5):1364–1368, Sep 1990.

[87] Steven Pennock and Zhixiang Wang. A tale of two cbls: Interplay of c-cbl and cbl-b in epidermal growth factor receptor downregulation. *Mol Cell Biol*, Mar 2008.

[88] J. Lippincott-Schwartz, L. Yuan, C. Tipper, M. Amherdt, L. Orci, and R. D. Klausner. Brefeldin A's effects on endosomes, lysosomes, and the TGN suggest a general mechanism for regulating organelle structure and membrane traffic. *Cell*, 67(3):601–616, Nov 1991.

[89] S. A. Wood, J. E. Park, and W. J. Brown. Brefeldin A causes a microtubule-mediated fusion of the trans-Golgi network and early endosomes. *Cell*, 67(3):591–600, Nov 1991.

[90] Yolanda R Carrasco, Maria N Navarro, and María L Toribio. A role for the cytoplasmic tail of the pre-T cell receptor (TCR) alpha chain in promoting constitutive internalization and degradation of the pre-TCR. *J Biol Chem*, 278(16):14507–14513, Apr 2003.

[91] Kristin A Hogquist, Troy A Baldwin, and Stephen C Jameson. Central tolerance: learning self-control in the thymus. *Nat Rev Immunol*, 5(10):772–782, Oct 2005.

[92] Alfred Singer. New perspectives on a developmental dilemma: the kinetic signaling model and the importance of signal duration for the cd4/cd8 lineage decision. *Curr Opin Immunol*, 14(2):207–215, Apr 2002.

[93] Myung-Shin Jeon, Alex Atfield, K. Venuprasad, Connie Krawczyk, Renu Sarao, Chris Elly, Chun Yang, Sudha Arya, Kurt Bachmaier, Leon Su, Dennis Bouchard, Russel Jones, Mathew Gronski, Pamela Ohashi, Teiji Wada, Debra Bloom, C. Garrison Fathman, Yun-Cai Liu, and Josef M Penninger. Essential role of the e3 ubiquitin ligase cbl-b in t cell anergy induction. *Immunity*, 21(2):167–177, Aug 2004.

[94] Natalia Jura and Dafna Bar-Sagi. Mapping cellular routes of ras: a ubiquitin trail. *Cell Cycle*, 5(23):2744–2747, Dec 2006.

[95] Debra A MacKenzie, Jill Schartner, Jack Lin, Amanda Timmel, Martha Jennens-Clough, C. Garrison Fathman, and Christine M Seroogy. Grail is up-regulated in cd4+ cd25+ t regulatory cells and is sufficient for conversion of t cells to a regulatory phenotype. *J Biol Chem*, 282(13):9696–9702, Mar 2007.

[96] Diana Gómez-Martín, Mariana Díaz-Zamudio, and Jorge Alcocer-Varela. Ubiquitination system and autoimmunity: The bridge towards the modulation of the immune response. *Autoimmun Rev*, 7(4):284–290, Feb 2008.

[97] Enrico Maggi, Lorenzo Cosmi, Francesco Liotta, Paola Romagnani, Sergio Romagnani, and Francesco Annunziato. Thymic regulatory t cells. *Autoimmun Rev*, 4(8):579–586, Nov 2005.

Curriculum vitae

(Darf aus Datenschutzgründen online nicht veröffentlicht werden.)

Posters, Talks and Publications

Posters

Re-Examination of the Role of ISG15 in Stat1-signaling and responses against Vesicular Stomatitis and Lymphocytic Choriomeningitis Virus in Isg15- and in Isg15/Ubp43-deficient mice, FMP and MDC PhD Retreat, Straussberg 2005.

Talks

Regulation of T cell development and immune function by the deubiquitinating enzyme UBPY, FMP and MDC PhD Retreat, Joachimsthal 2007.

Publications

Knobeloch KP, Utermohlen O, Kisser A, Prinz M, Horak I. *Reexamination of the role of ubiquitin-like modifier ISG15 in the phenotype of UBP43-deficient mice*, Mol Cell Biol. 2005

Niendorf S, Oksche A, Kisser A, Lohler J, Prinz M, Schorle H, Feller S, Lewitzky M, Horak I, Knobeloch KP. *Essential role of Ubiquitin specific protease 8 (UBPy) for receptor tyrosine kinase stability and endocytic trafficking in vivo*, Mol Cell Biol. 2007

Acknowledgements

First of all I wish to thank Prof.Dr.Ivan Horak and Dr.Klaus-Peter Knobeloch for giving me the opportunity to work on this project and for continuous support during this time.

I want to thank Dr.Sandra Niendorf for building the fundaments of this work.

I also would like to reward Prof.Dr.Christoph Loddenkemper and Dr.Ulrich Steinhoff for helping with the analysis of the colitis.

To Prof. Dr. Hartmut Oschkinat I would like to thank for evaluating this thesis.

I am very grateful to my colleagues from the department for providing an inspiring working environment, for friendly discussions and useful suggestions.

I owe my warm thanks to Claudia Pallasch and Bianca Wittig for expert care about transgenic mice, Markus Wietstruk for skilful technical assistance and Alexandra Kiesling for managing the administrative struggles.

Lastly I also want to thank the diploma students who helped in this project, Stephanie Manthey and Carolin Westendorf, for their excellent results.